



OPEN

## Anti-inflammatory effects of $^{64}\text{Zn}$ -aspartate is accompanied by cognitive improvements in rats with $\text{A}\beta_{1-40}$ -induced alzheimer disease

Max Temnik<sup>1</sup>, Mariia Rudyk<sup>2</sup>✉, Alexandr Balakin<sup>1</sup>, Sergey Gurin<sup>1</sup>, Taisa Dovbynychuk<sup>2</sup>, Roman Byshovets<sup>3</sup>, Nataliia Dzubenko<sup>4</sup>, Ganna Tolstanova<sup>4</sup> & Larysa Skivka<sup>2</sup>

Alzheimer disease (AD) is a debilitating progressive dementia, whose pathophysiology is not fully understood. Chronic inflammation is now widely accepted as one of the key features of AD pathogenesis. Because of this, anti-inflammatory preparations are considered as putative disease modifying agents. A new compound of zinc aspartate with enriched light atoms  $^{64}\text{Zn}$  ( $^{64}\text{Zn}$ -asp) was evaluated as a possible anti-AD agent using  $\text{A}\beta_{1-40}$ -induced AD model. Intrahippocampal  $\text{A}\beta_{1-40}$  injection resulted in pronounced neuroinflammation, as was evidenced by increased phagocytic activity, augmented reactive oxygen species generation, and up-regulated CD86 and CD206 expression by microglia. In rats with  $\text{A}\beta_{1-40}$ -induced AD, persistent systemic inflammation was also registered, as was ascertained by significantly increased white blood cell-based inflammatory indices and development of anemia of inflammation. Neuro- and systemic inflammation in rats was accompanied by hippocampal dopamine neuron loss, as well as by impairment of short-term and remote spatial memory and cognitive flexibility. Intravenous  $^{64}\text{Zn}$ -asp administration rats with AD was associated with returning all microglia indicators to normal range. All aforementioned features of systemic inflammation were not observed in these animals. Anti-inflammatory  $^{64}\text{Zn}$ -asp effect was strongly correlated with improvement of short-term spatial memory and cognitive flexibility, and moderately—with betterment of remote spatial memory. These results demonstrated that i.v.  $^{64}\text{Zn}$ -asp administration could reverse the inflammatory and, as a result, cognitive effects of intra-hippocampal  $\text{A}\beta_{1-40}$  in rats. Therefore, its use may be a viable approach in the complex therapeutic strategy for AD.

**Keywords** Alzheimer disease, Stable light isotope enriched zinc aspartate, Anti-inflammatory agent, Inflammation, Neuroinflammation, Cognitive improvement

Alzheimer's disease (AD) is the most prevalent type of dementia, which is defined as slowly progressive neurodegenerative disease associated with neuronal death, memory deficits and cognitive impairment<sup>1,2</sup>. Considering the rapid increase of the global ageing population, the age-related disorders, especially AD, are an earnest threat to the public health. In the US, the number of AD patients is expected to grow to 13.8 million by 2060<sup>3,4</sup>. In Europe, based on current predictions, the population in 2080 will be 520 million with 13.7 million patients with AD<sup>5</sup>.

There are no effective disease-modifying drugs for AD treatment, mostly because the underlying causes of sporadic disease remain incompletely understood. Key AD pathological features include the accumulation of extracellular amyloid  $\beta$  ( $\text{A}\beta$ ) plaques and intraneuronal neurofibrillary tangles of phosphorylated tau protein (tau/NFT)<sup>6</sup>. Four FDA approved preparations: acetylcholinesterase inhibitors (donepezil, galantamine, and rivastigmine) and a N-methyl D-aspartate receptor ion channel antagonist memantine do not provide a cure,

<sup>1</sup>Physical Chemistry, Vector Vitale, North Miami Beach, USA. <sup>2</sup>Educational and Scientific Centre "Institute of Biology and Medicine", Taras Shevchenko National University of Kyiv, 2, Hlushkova Avenue, Kyiv 03022, Ukraine.

<sup>3</sup>Department of Internal Diseases, Bogomolets National Medical University, 13, Shevchenko Blvd., Kyiv 01004, Ukraine. <sup>4</sup>Educational and Scientific Institute of High Technologies, Taras Shevchenko National University of Kyiv, 4g, Hlushkova Avenue, Kyiv 03022, Ukraine. ✉email: rudyk\_marie@knu.ua

but rather limit the symptoms of the disease. Monoclonal antibodies that target A $\beta$  plaques (aducanumab, lecanemab and donanemab) have shown potential in reducing their deposition and slowing cognitive decline in clinical trials. However, the use of these drugs is associated with adverse immune responses.<sup>7–9</sup> Considering a serious demand for disease-modifying drugs, main efforts are focused on finding new therapeutic targets in the context of available knowledge concerning AD pathogenesis. According to current hypotheses, amyloid cascade<sup>10</sup>, oxidative stress<sup>11</sup>, and cerebral amyloid angiopathy<sup>12</sup> are regarded main pathogenesis components.

Lately, inflammation (peripheral and central or neuroinflammation) is considered a novel AD feature and potential therapeutic target<sup>13–15</sup>. The use of non-steroidal anti-inflammatory drugs have not been successful in treating AD<sup>16</sup>. Other drugs targeting inflammation resolution and restoration of microglia phagocytic function for effective A $\beta$  clearance are presently being tested (TNF- $\alpha$  blocker etanercept, COX-1 inhibitor CSP-1103 etc.) with promising results<sup>8</sup>.

Inflammation is associated with a range of biochemical responses, which in turn provokes alterations in levels of acute phase reactants including zinc concentration<sup>17</sup>. Zinc is the second most plentiful trace element in the human central nervous system. The brain is known to have significant zinc content, particularly in specific synaptic vesicles of glutamatergic neurons. Zinc homeostasis is highly important for healthy brain function, since this trace element is a structural component in ~70% of proteins. Zinc is involved in the functioning of more than 300 enzymes, 2000 transcription factors, and is crucial for numerous neurobiological processes<sup>18</sup>. Zinc dyshomeostasis is involved in the pathophysiology of chronic diseases related to aging, since the intestinal zinc absorption is declined with age<sup>19</sup>. Zinc dysregulation violates neural networks and supports pathological events, potentially leading to neurodegeneration. Moreover, emerging evidence demonstrated that zinc is involved in key aspects of AD pathogenesis: A $\beta$  plaques and tau/NFT formation<sup>20</sup>. All these facts stipulated formulating zinc dyshomeostasis hypothesis of AD, which is closely related to inflammation<sup>21</sup>.

Zinc levels have been extensively investigated in different brain regions, as well as in serum and plasma in patients with AD and in animal models of the disease. Studies concerning serum/plasma zinc levels in AD patients exhibited contradictory results. Numerous human studies have demonstrated that serum zinc levels are lower in individuals with mild to moderate AD dementia (ranging from 0.5 to 2 on the Clinical Dementia Rating scale) compared to healthy controls. Moreover, reduced serum zinc levels have been associated with the rapid progression of AD dementia and cognitive decline<sup>22</sup>. However, González et al. (1999) reported a significant increase in serum zinc levels in patients with late-onset AD compared to healthy controls<sup>23</sup>. Similarly, findings by Rembach et al. (2014) showed no significant differences in serum zinc levels between AD patients and healthy individuals, leading the authors to conclude that decreased serum zinc is a consequence of aging rather than AD<sup>24</sup>. There is also no consensus about the zinc content in AD brains. Post-mortem analyses of AD brains showed both decreased zinc levels in brain tissue<sup>25</sup> and significantly increased zinc levels in the hippocampus and amygdala<sup>26</sup> as compared to healthy controls. Nevertheless, it is commonly accepted that pathological changes glutamatergic activation in AD leads to synaptic zinc dyshomeostasis, which in turn causes microglia activation. Microglia has recently been recognized as an important contributor in AD pathogenesis. Microglia is a population of tissue-resident macrophages in the brain, which are responsible for sustaining, nourishing, and immune surveillance<sup>27</sup>. However, pro-inflammatory disease-associated microglia (DAM) drives neuroinflammation, which contributes to AD initiation/progression and severity, and microglia-targeted therapeutics could be promising in mitigating neuroinflammatory responses<sup>28</sup>. Zinc plays important roles in microglia activation and can cause either pro-inflammatory (AD promoting) or anti-inflammatory metabolic shift of these cells depending on their initial activation state. In particular, under conditions of a pro-inflammatory metabolic shift in microglia, zinc inhibits the inflammatory responses of these cells<sup>29,30</sup>. These anti-inflammatory effects of zinc are mediated through multiple mechanisms. It mitigates oxidative stress over the long term by inducing the expression of metallothioneins—cysteine-rich proteins with electron-scavenging and cytoprotective properties<sup>31</sup>. Research has shown that restoring physiological zinc levels suppresses immune activation, whereas zinc deficiency, particularly in the presence of immune activation, leads to a systemic increase in NF- $\kappa$ B activation, exacerbating inflammation. Zinc inhibits NF- $\kappa$ B activation and its downstream pro-inflammatory genes, such as tumor necrosis alpha (TNF- $\alpha$ ) and interleukin 1 beta (IL-1 $\beta$ ), while upregulating A20 and Peroxisome Proliferator-Activated Receptor alpha (PPAR- $\alpha$ )—two zinc-finger proteins with known anti-inflammatory properties. Another pathway involves the inhibition of cyclic nucleotide phosphodiesterase, which also contributes to NF- $\kappa$ B suppression. Additionally, zinc ions transported into cells via ZIP8 are believed to inhibit I $\kappa$ B kinase, further attenuating the inflammatory response<sup>32</sup>.

Since zinc dyshomeostasis is involved in AD and associated with inflammation, numerous dietary zinc supplementation studies were performed in mice and humans with no clear consensus on the effects of zinc supplementation in AD pathology in animal models<sup>24</sup>. However, improvements in cognition and memory in AD patients following dietary zinc supplementation were reported in a few clinical trials<sup>33,34</sup>. In all these studies, isotopically natural zinc compounds were used. Zinc has five stable isotopes (<sup>64</sup>Zn, <sup>66</sup>Zn, <sup>67</sup>Zn, <sup>68</sup>Zn, and <sup>70</sup>Zn) with average natural abundances of 48.6, 27.9, 4.1, 18.8, and 0.6% respectively. Since the isotopes <sup>64</sup>Zn and <sup>66</sup>Zn are the most abundant, the ratio of <sup>66</sup>Zn/<sup>64</sup>Zn expressed as  $\delta^{66}\text{Zn}$  is commonly used for characterizing Zn isotopic compositions in mammalian tissues<sup>35</sup>. One of the features of zinc homeostasis in healthy brain is the prevalence of light isotope <sup>64</sup>Zn ( $\delta^{66}\text{Zn} < 1$ )<sup>36</sup>. This predominance is explained by the peculiarities of chemical bonds of zinc in its compounds in different tissues. Zinc bonds with oxygen- (sulfate, phosphate, lactate) and nitrogen-containing motifs (histidine) is tight and facilitate heavy isotope, whereas bonds with sulfur (cysteine, methionine) favor light zinc isotope. In healthy brain, zinc is mostly bound to cysteine within metallothioneins<sup>37,38</sup>. According to current hypothesis, heavy zinc isotope accumulates through time in the human body, and  $\delta^{66}\text{Zn}$  increases with age<sup>35,39</sup>. This re-distribution of zinc isotopes in the brain is manifested in neurological diseases associated with protein misfolding<sup>36</sup>. Namely, in AD brains, particularly in amyloid- $\beta$

(A $\beta$ ) plaques, heavy zinc isotope binds to the histidine residues in the N-terminal hydrophilic region of the A $\beta$  peptide.

In this study, we used novel zinc-based drug substance, KLS-1, which is zinc aspartate enriched with light isotope  $^{64}\text{Zn}$  to 99.2% atomic fraction of total zinc (as opposed to the natural isotopic ratio of 48.6% used in zinc supplements). In our previous experiments,  $^{64}\text{Zn}$  aspartate ( $^{64}\text{Zn}$ -asp) demonstrated greater biological activity, including a stronger effect on NF- $\kappa$ B expression, compared to Zn aspartate with a natural isotope distribution<sup>40,41</sup>. A possible explanation for these findings is the increased affinity of the light zinc isotope for cysteine, which is abundant in proteins involved in zinc metabolism, such as metallothioneins, Zrt- and Irt-like proteins (ZIP), and zinc transporters<sup>42</sup>. This gave grounds to assume that  $^{64}\text{Zn}$ -asp would possess potent anti-inflammatory properties.

Usually, zinc supplements are given orally with weak therapeutic efficacy. Aforementioned decline of intestinal zinc absorption with age could be one of the reasons, and parenteral supplementation could eliminate this drawback<sup>43–45</sup>. To our best knowledge, this is a first report concerning the impact of intravenous (i.v.) administration of isotopically modified zinc in animal model of AD. The aim of this study was to assess the effect of  $^{64}\text{Zn}$ -asp (KLS-1) i.v. administration on local and systemic inflammation, as well as on cognitive parameters in rats with A $\beta_{1-40}$ -induced AD.

## Materials and methods

### Test agent

$^{64}\text{Zn}$ -asp (KLS-1), an investigational new complex of zinc aspartate containing a Zn atom enriched in light isotope  $^{64}\text{Zn}$  to >99% atomic fraction of total zinc. (Fig. 1), was used as a therapeutic test agent. Molecular formula:  $\text{C}_8\text{H}_{12}\text{O}_8\text{N}_2\ ^{64}\text{Zn}$ .

For the animal study, the  $^{64}\text{Zn}$ -asp solution was prepared ex tempore, right before administration, with a zinc concentration of 6.75 mg/mL. Water for injection served as the diluent.

### Animals and study design

Study design is provided in Fig. 2. A total of 32 male Wistar rats (14 months old, 400–500 g) were utilized in the study. Animals were provided by L.I. Medved's Research Center of Preventive Toxicology, Food and Chemical Safety, Ministry of Health, Ukraine Center for Preventive, and regulatory toxicology (Kyiv, Ukraine, GLP statement No G-042). Animals were held in the vivarium of the ESC "Institute of Biology and Medicine" of Taras Shevchenko National University of Kyiv in standard conditions (temperature  $20 \pm 2$  °C, 12 h light/dark cycle with free access to water and food). Each rat was kept in a separate cage. The animal maintenance protocol was approved by the University's Bioethics Committee in accordance with the Animal Protection Act (protocol No 4, 10.10.2022). All animal studies were performed in accordance with the norms established by the Law of Ukraine No. 3447-IV "On the Protection of Animals from Cruelty", and in accordance with the standards of the Convention on Bioethics of the Council of Europe "European Convention for the Protection of Vertebrate Animals Used in Experimental and Other Scientific Research goals" (1997), general ethical principles of work with experimental animals approved by the First National Congress on Bioethics of Ukraine (September 2001) and other international agreements and national legislation in this field. All procedures in this study were conducted in accordance with the ARRIVE guidelines.

Before the experiment, the animals were randomly distributed into 4 groups (Fig. 2A) using the "RAND ()" function in Microsoft Excel: I (n=8) – intact animals, which did not undergo any manipulations (intact); II (n=8) – sham-operated (sham) animals; III (n=8) – rats with A $\beta_{1-40}$  induced AD (AD), and IV (n=8) – AD animals received 10 daily i.v. (into the lateral tail vein)  $^{64}\text{Zn}$ -asp injections at a dose of 1.5 mg/kg (0.1 ml of the stock solution) starting from the Day 18. Behavioral testing was performed as illustrated in Fig. 2B and detailed in Section "Behavioral testing".

On Day 37, rats were euthanized via carbon dioxide inhalation followed by cervical dislocation<sup>46</sup>, and biological samples (brain tissue and blood) were collected for immunohistochemistry, ELISA, as well as hematological and immunological analyses.



**Fig. 1.** Schematic representation of  $^{64}\text{Zn}$ -Aspartate structure.

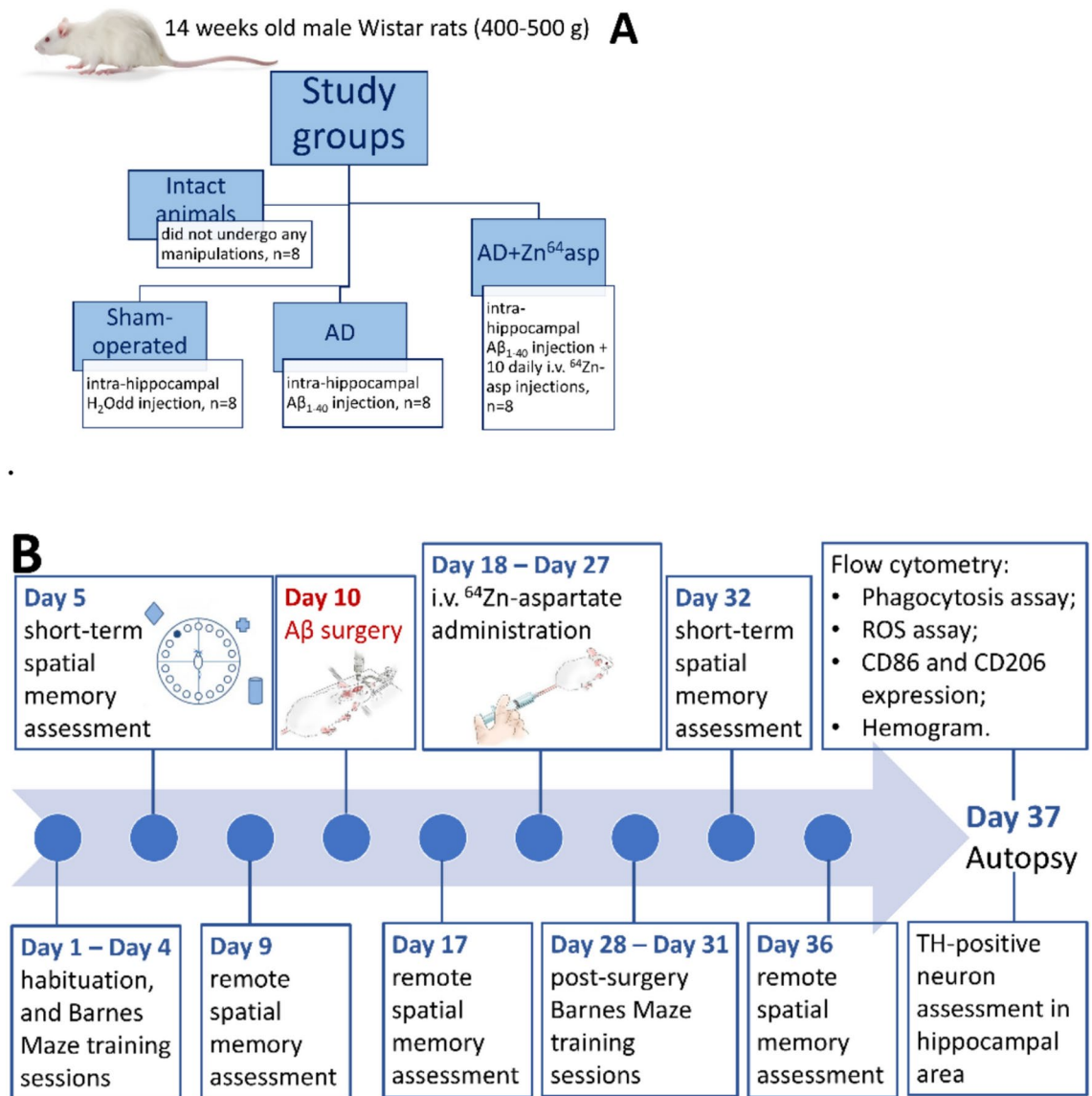


**Fig. 2.** Animal groups (A) and study design (B).

### A $\beta_{1-40}$ -induced AD model

A $\beta_{1-40}$  (Cayman Chemical, USA) solution was dissolved in ddH<sub>2</sub>O at a concentration of 15  $\mu$ mol/L and incubated at 37 °C for 24 h before use. Surgery and A $\beta_{1-40}$  AD induction were performed as described previously<sup>47–49</sup>. Rats were anesthetized with a mixture of ketamine (75 mg/kg, Sigma, USA) and 2% xylazine (100  $\mu$ L/rat, Alfasan International B.V., The Netherlands) i.p. in the volume of 1 mL<sup>50</sup>. After this, rats were placed in a stereotaxic apparatus (SEJ-4, Ukraine), and were scalped from the point of intersection of the sagittal suture with the bregma (zero point): 2 mm distally, 2 mm laterally, and 3.5 mm deep, and a burr hole was made with an injection needle directly into the hippocampus. Then, rats were injected unilaterally into hippocampus with aggregated A $\beta_{1-40}$ . The volume of the suspension was 10  $\mu$ L per rat, infusion was made for 5 min at a rate of 0.5  $\mu$ L/min (every 15 s). After A $\beta$  infusion, the tip of the microinjector stayed in the brain tissue for 4 min. Sequentially, the microinjector was removed, and the soft tissues of the head were sutured. The sham group received intra-hippocampal injection of 10  $\mu$ L of sterile ddH<sub>2</sub>O<sup>49</sup>.

### Behavioral testing

To evaluate hippocampal-dependent learning, short-term and long-term (remote) spatial memory, the Barnes maze was used<sup>51</sup>. The testing was aimed in estimating the animal ability to learn and memorize the location of the escape box using visual hints on the walls around the device. Barnes maze consisted of a rotative platform (120 cm in diameter), raised 90 cm above the floor. The platform contained 16 escape holes (each is 10 cm in diameter) located along its periphery. Spatial hints (black triangles and paired black stripes) were placed on the walls of the room to serve as visual cues for navigation and spatial orientation during the Barnes maze test. A

dark escape box with a standard animal filler was put under the target hole. Each animal was assigned its own target escape box number. The habituation trial and training phase consisted of a set of four 3–5 min daily training sessions (each with four trials per day with 15-min intertrial interval). Just before each trial, the animals were placed inside a dark starting cylinder positioned at the center of the platform for 10 s. Sequentially, the cylinder was removed, and animals were permitted to explore the maze and holes for 2–3 min, or until they found the target hole. If the animal failed to find the box within this time period, it was guided lightly to the target hole. On Day 5 (24 h after the last training), the short-term spatial memory was tested, and on Day 9 (5th day after the last training), after the memory consolidation period, the remote memory was tested: the escape box was removed from the maze, and the entrance to the escape box was closed. The rats were given 90 s of free movement across the platform for finding the entrance to its own target hole (where the entrance to the escape box was previously located), based on previously gained skills. On Day 10, the  $A\beta_{1-40}$  induction surgery was performed as described above. On Day 17 (7 days after the surgery) remote spatial memory was tested again. From Day 28 to Day 31 (18 to 21 days after the surgery), the animals were retrained (the escape box for each animal was relocated), and post-surgery short-term and remote memory were assessed on Day 32 and Day 36 after the intrahippocampal  $A\beta$  infusion respectively. During testing, cognitive activity was recorded using a digital camera (“Casio® EX-Z850,” China) positioned 1 m above the center of the platform, followed by analysis in MATLAB. The test endpoints were (in seconds): 1) escape latency—the time required for an animal to find the entrance to the target escape box from when the animal is released from the starting cylinder (characterizes spatial learning and spatial memory—related to the function of the hippocampus) –  $t_1$ ; 2) the time spent near the entrance to closed target hole (characterizes cognitive flexibility—related to the function of the frontal cortex of the brain<sup>52</sup> –  $t_2$ . In addition,  $\Delta t_{1-5-32}$  and  $\Delta t_{2-5-32}$  were calculated for assessing changes in short-term spatial memory and cognitive flexibility in the course of AD and after the treatment with  $^{64}\text{Zn}$ -asp.  $\Delta t_{1-9-17}$ ,  $\Delta t_{1-9-36}$ ,  $\Delta t_{2-9-17}$  and  $\Delta t_{2-9-36}$  were also calculated for assessing changes in remote spatial memory and cognitive flexibility.

### Immunohistochemistry

Dopaminergic neuron (DN) degeneration in hippocampal area was evaluated by immunohistochemical staining of tyrosine hydroxylase (TH)-positive neurons<sup>53</sup>. Profoundly anaesthetized rats were transcardially perfused with ice-cold heparinized saline (5000 U/L), and then with 4% paraformaldehyde. After this, animal brains were gently excised and fixed in 4% paraformaldehyde overnight. For immunohistochemical staining 5  $\mu\text{m}$ -thick sections were used. Endogenous peroxidase activity was quenched with blocking solution (Dako, EnVision Flex, DM821). Nonspecific secondary antibody binding was blocked with a 4% solution of milk powder in Tris-buffered saline (TBS) with 0.2% Triton X-100. First, tissue sections were incubated with primary antibody (dilution 1:200 in TBS with 0.2% Triton X-100) (Millipore, AB152) at 4 °C overnight. After this, the sections were incubated with secondary antibody (biotinylated anti-rabbit, 1:200) for 60 min, and then—with a streptavidin–biotin horseradish peroxidase solution. Immunolabelling was visualized using 0.5% solution of diaminobenzidine tetrahydrochloride in TBS containing 30% hydrogen peroxide (Dako, EnVision). Immunostained section photomicrographs were analyzed using ImageJ software (1.54f, the 32-bit version, <https://imagej.net/ij/>, USA). TH-positive staining intensity was assessed using a Quantitative Scoring Methods, considering the number of positive (stained) cells and staining intensity<sup>54</sup>. The results were counted by multiplying the percentage of positive cells (P) by the intensity (I) and presented as a quick estimate (Q):  $Q = P \times I$ .

### $A\beta_{40}$ ELISA in hippocampal homogenates

For the analysis of  $A\beta_{40}$ , the hippocampus was isolated and homogenized in an ice-cold 10% (w/v) phosphate-buffered saline (PBS) solution (0.1 M, pH 7.4) supplemented with a protease inhibitor cocktail, and centrifuged at  $21,000 \times g$  for 45 min at 4 °C. The obtained supernatant was collected, while the remaining pellet was resuspended in 70% formic acid at 4 °C and centrifuged again under identical conditions for 2 h. The formic acid extracts were neutralized using a 1 M Tris–phosphate buffer (pH 11) at a 1:20 ratio. The final supernatant was collected and preserved at –80 °C until further analysis. The  $A\beta_{40}$  concentration was measured using ELISA kits, following the manufacturer’s instructions (Cloud-Clone Corp., China)<sup>55</sup>.

### Hematological assay

EDTA anti-coagulated blood was used in hematological investigations. The hematological indices were determined using an automated hematology analyzer “Particle counter model PCE 210” (ERMA, Japan), adapted for the study of blood cells of rats and mice. Neutrophil to lymphocyte ratio (NLR), lymphocyte to monocyte ratio (LMR), platelet to lymphocyte ratio (PLR), platelet to neutrophil ratio (PNR), platelet to monocyte ratio (PMR), neutrophil to monocyte ratio (NMR), systemic immune inflammation index (SII), and a mean platelet volume (MPV)/ platelet count (PLT) were calculated using the following formulas:  $NLR = \text{absolute neutrophil count (ANC)}/\text{absolute lymphocyte count (ALC)}$ ;  $LMR = \text{ALC}/\text{absolute monocyte count (AMC)}$ ;  $PLR = \text{absolute platelet count (APC)}/\text{ALC}$ ;  $PNR = \text{APC}/\text{ANC}$ ;  $PMR = \text{APC}/\text{AMC}$ ;  $NMR = \text{ANC}/\text{AMC}$ ;  $SII = (\text{ANC} \times \text{APC})/\text{ALC}$ <sup>56</sup>. Additionally, a mean platelet volume (MPV)/ platelet count (PLT) was calculated.

### Microglia/macrophage cell isolation

Complex population of microglia/macrophage cells was isolated as described by Frank et al.<sup>57</sup> with slight modifications<sup>49,58</sup>. Whole brain was lodged in cold Dulbecco’s PBS (DPBS) supplemented with 0.2% glucose and minced into 1–2 mm pieces using scissors. After this, tissue pieces were carefully disintegrated in DPBS using a tissue homogenizer. For separating cell aggregates, homogenate was filtered through a 40  $\mu\text{m}$  cell strainer (BD Biosciences Discovery, USA), and cell suspension was then centrifuged at 350 g for 10 min. Cells were then mixed with 1 ml of 70% isotonic Percoll (Sigma). Two milliliters of 50% isotonic Percoll was carefully layered on top of the 70% layer followed by 1 ml PBS layering on the top of the 50% Percoll layer. prepared mixture was then

centrifuged at 1200 g for 45 min. The layer enriched with microglia/macrophages at the interface between the 70 and 50% isotonic Percoll phases were isolated. Cell viability was assessed using the trypan blue exclusion test. The proportion of viable cells was  $\geq 95\%$ . FITC-conjugated mouse anti-rat CD11b antibodies (BD Pharmingen, USA) and PE-conjugated mouse anti-rat CD45 (BD Pharmingen, USA) were then used for assessing cell purity. CD11b + CD45 + cell proportion was  $\geq 88\%$ .

### Flow cytometry

Flow cytometry was used for assessing polarized activation of phagocytes: microglia/macrophage cells and peripheral blood monocytes (Mo) and granulocytes (Gr), which was characterized by phagocytic activity, reactive oxygen species generation and expression of phenotypic markers CD206 and CD86 as described earlier<sup>49,58</sup>. In the phagocytic activity assay, FITC-labeled thermally inactivated cells of *Staphylococcus aureus* Cowan I (collection of the Department of Microbiology and Immunology, ESC "Institute of Biology and Medicine" of Taras Shevchenko National University of Kyiv) were used as an endocytosis object. Isolated microglia/macrophage cells or animal blood samples were incubated with bacterial cells for 30 min at 37 °C. Phagocytosis was stopped using a 'stop' solution (PBS with 0.02% EDTA and 0.04% paraformaldehyde). Data are presented as the phagocytosis percentage (PP) and phagocytosis index (PI) (the mean fluorescence intensity, MFI). The oxidative metabolism was tested using 2',7'-dichlorodihydrofluorescein diacetate (H2DCFDA, Invitrogen). Data are presented as percentage of ROS-producing cells and ROS generation level (the mean fluorescence intensity, MFI). FITC-labeled anti-CD86, and phycoerythrin (PE)-labeled anti-CD206 antibodies (Becton Dickinson, Pharmingen, USA) were used for phagocyte phenotyping. Results were assessed using DxFlex flow cytometer and analyzed using Kaluza C Analysis Software (Beckman Coulter, Inc., USA, C10574, <https://www.beckman.ua/flow-cytometry/software/kaluza-c/c10574>). Gr and Mo were gated according to forward and side scatter.

### Statistical analysis

Statistical analysis was conducted using the Statistica 12.0 package. First, data was examined for normality of distribution using the Shapiro–Wilk test<sup>59</sup>. Normally distributed variables are expressed as mean  $\pm$  SD. Nonnormally distributed variables are expressed as the median and interquartile range (IQR). Statistical differences were calculated using ANOVA with Tukey's post-hoc test for multiple comparisons of variables with a normal distribution, and Kruskal–Wallis's test for multiple comparisons of variables with a non-normal distribution<sup>60</sup>. Spearman correlation test was used to determine the statistical relationships between the short-term and remote spatial memory parameters and inflammation biomarker values. Differences were considered significant at  $p < 0.05$ .

## Results

### *Treatment with <sup>64</sup>Zn-asp abrogates pro-inflammatory metabolic polarization of microglia/macrophage population in rats with A $\beta$ <sub>1-40</sub>-induced AD*

In our experiments, complex population of microglia (MG)/border-associated macrophages (BAM) were examined. In healthy brain of intact animals, yolk sac-derived resident microglial cells (MG) prevail with minor fraction of border-associated macrophages (BAM). Aging in human and rodents is associated with an increase in the proportion of BAM in the complex population of brain phagocytes, and with their slight pro-inflammatory shift caused by age-associated low-grade inflammation<sup>61</sup>. In addition, in neurodegeneration, BAM fraction can increase as a result of blood monocytes recruitment<sup>62</sup>. Phagocyte polarized activation was assessed by key functional characteristics, which allow to evaluate their metabolic shift (pro- or anti-inflammatory): phagocytic activity, oxidative metabolism and expression of phenotypic markers CD86 and CD206<sup>63</sup>. It is necessary to note, that MG/BAM population in sham-operated animals was in activated state, as indicated by increased phagocytic activity (which was characterized by PI values) as compared to intact animals (Fig. 3B). ROS generation was also higher in MG/BAM from rats in sham group than in intact animals (Fig. 3C). This can be attributed to residual low-grade inflammation after the placebo neurosurgery. Nevertheless, proportion of phagocytizing MG/BAM cells in sham-operated animals was even lower than that in intact animals (Fig. 3A), indicating the resolution of post-surgery meta-inflammation and returning MG/BAM cells to resting state. Fractions of CD86 + (Fig. 3D) cells and CD206 + cells (Fig. 3F), as well as expression levels of these phenotypic markers (Fig. 3E and G correspondingly) in MG/BA population of sham-operated rats did not differ significantly from those in intact animals, additionally evidencing a lack of pronounced inflammation.

MG/BAM population in rats with A $\beta$ <sub>1-40</sub>-induced AD had all the hallmarks of activated and pro-inflammatory shifted cells. Median value of PP (proportion of phagocytizing cells) was 2.6 times higher as compared to intact rats and almost 10 times higher than in sham-operated group (Fig. 3A). Median value of PI in AD rats was 6 times higher as compared with intact animals and 3 times higher than in rats from sham group (Fig. 3B). Levels of ROS production by MG/BAM in animals with AD were 2.5 times higher as compared to those in sham-operated rats and 5 times higher than in intact animals (Fig. 3C). Our next parameter, CD86 is one of the co-stimulatory molecules, which is constitutively expressed by all tissue-resident macrophages including MG. Overexpression of CD86 is associated with pro-inflammatory shift of macrophage profile. In our experiments, proportions of CD86 + MG/BAM did not differ significantly in all animal groups (Fig. 3D), although median value of this parameter in rats with A $\beta$ <sub>1-40</sub>-induced AD was almost twice as high as in control animals. CD86 expression levels in AD animals were 3 times higher as compared to control rats (Fig. 3E). Our next indicator—CD206—is a key phenotypic marker differentiating MG and BAM, since resting MG is CD206 negative, reactive microglia (which is involved in neuroinflammation and AD pathogenesis) is CD206<sup>low</sup>, whereas BAM are CD206<sup>high</sup><sup>64,65</sup>. Median value of the proportion of CD206 + cells in MG/BAM population from rats with AD was three times higher than that in control animals indicating increase of BAM fraction and/or resident MG

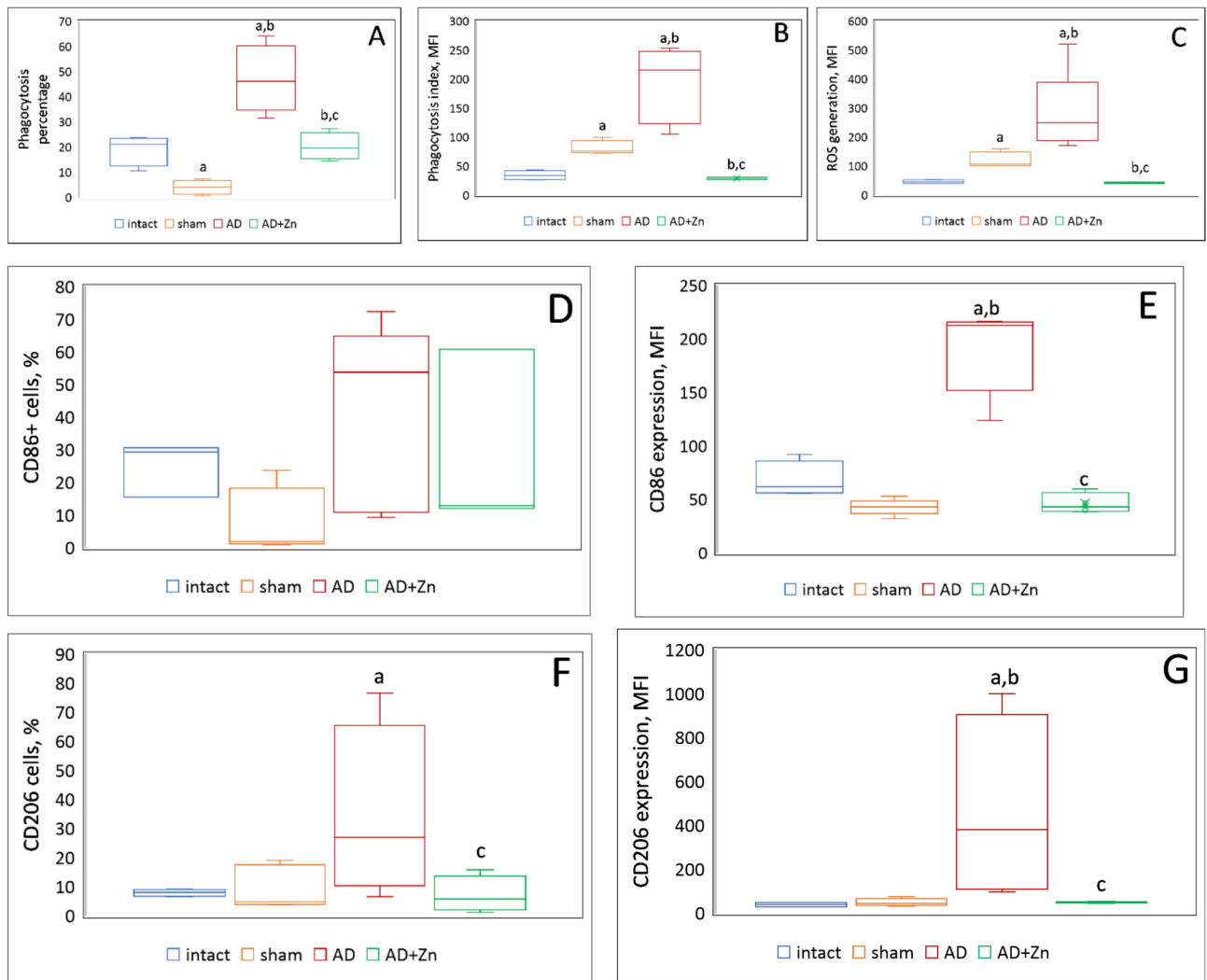


**Fig. 3.** Effect of i.v. administration with  $Zn^{64}$ -asp on metabolic characteristics of microglia/macrophages in rats with  $A\beta_{1-40}$ -induced AD. A – phagocytosis percentage; B – phagocytosis index; C – ROS generation; D – fraction of CD86-positive cells; E – CD86 expression level; F – fraction of CD206-positive cells; G – CD206 expression level. Data are presented as medians and IQR. Data from different animal groups were compared using Kruskal–Wallis’s test. **a**— $p \leq 0.05$  as compared to intact animals, **b**— $p \leq 0.05$  as compared to sham-operated animals; **c**— $p \leq 0.05$  as compared to animals with  $A\beta_{1-40}$ -induced AD.

activation (Fig. 3F). Median value of CD206 expression level in rats with  $A\beta_{1-40}$ -induced AD was nearly 10 times higher than in control animals (Fig. 3G).

Treatment rats with  $A\beta_{1-40}$ -induced AD with  $^{64}Zn$ -asp returned all MG/BAM indicators to normal range. PP values of MG/BAM in this group were at the level of intact animals (Fig. 3A). Phagocytic activity (Fig. 3B) and ROS generation (Fig. 3C) values were also the same as in intact rats. Of special note is low individual variability of these indicators in rats with AD treated with  $^{64}Zn$ -asp, which provided the high significance of differences in comparison with untreated rats with AD. As mentioned above, percentage of CD86+ cells in MG/BAM population was similar in all animal groups. Nevertheless, median value of this indicator in rats with AD treated with  $^{64}Zn$ -asp was 4 times lower than that in untreated AD animals, and was even lower than in intact animals (Fig. 3D). CD86 expression levels in rats with  $A\beta_{1-40}$ -induced AD received i.v. zinc administration was 5 times lower as compared to values of untreated animals with AD and was the same as in sham-operated rats (Fig. 3E). Percentage of CD206+ cells in MG/BAM population in AD rats received i.v. zinc was 5 times lower than in untreated animals and did not differ from that in sham-operated rats (Fig. 3F). Median value of CD206 expression level on rats treated with  $^{64}Zn$ -asp was 8 times lower than in untreated AD animals and did not differ from those in control groups (Fig. 3G).

### ***$^{64}Zn$ -asp mitigates systemic inflammation in rats with $A\beta_{1-40}$ -induced AD***

Pro-inflammatory MG/BAM activation in rats with  $A\beta_{1-40}$ -induced AD was also accompanied by persistent systemic inflammation, as ascertained by commonly accepted hematological markers<sup>66</sup>: apparent leukocytosis (WBC count was twice higher as compared to intact animals, and 1.3 times higher than in sham-operated rats)

	Intact animals, n = 8	Sham-operated animals, n = 8	A $\beta_{1-40}$ -induced AD, n = 8	A $\beta_{1-40}$ -induced AD + $^{64}\text{Zn-asp}$ , n = 8
WBC, $\times 10^3/\mu\text{l}$	12.4 [10.5; 14.9]	19.3 [17; 24] <sup>a</sup>	24.3 [23.9; 24.7] <sup>ab</sup>	13.7 [10.1; 20] <sup>c</sup>
Ly, $\times 10^3/\mu\text{l}$	5.3 $\pm$ 2.1	10.5 $\pm$ 4.7	4.5 $\pm$ 0.2	6.2 $\pm$ 2.8
Mo, $\times 10^3/\mu\text{l}$	1.5 $\pm$ 0.5	2.2 $\pm$ 0.4	0.2 $\pm$ 0.05 <sup>ab</sup>	1.3 $\pm$ 0.6 <sup>c</sup>
Gr, $\times 10^3/\mu\text{l}$	4.2 $\pm$ 1.2	6.7 $\pm$ 2.2	19.6 $\pm$ 0.7 <sup>ab</sup>	6.2 $\pm$ 2.4 <sup>c</sup>
PLT, $\times 10^3/\mu\text{l}$	225.5 $\pm$ 28.7	397.7 $\pm$ 93 <sup>a</sup>	401.6 $\pm$ 29.4 <sup>a</sup>	255 $\pm$ 37.5 <sup>bc</sup>
Ly, %	60.0 $\pm$ 12.8	53.2 $\pm$ 4.7	18.3 $\pm$ 0.5 <sup>ab</sup>	50.6 $\pm$ 5.9 <sup>c</sup>
Mo, %	8.4 $\pm$ 2.8	10.8 $\pm$ 3.8	0.9 $\pm$ 0.2 <sup>ab</sup>	7.5 $\pm$ 2.5 <sup>c</sup>
Gr, %	39.7 $\pm$ 9.5	36 $\pm$ 4.5	80.6 $\pm$ 0.4 <sup>ab</sup>	41.9 $\pm$ 7.4 <sup>c</sup>

**Table 1.** WBC count with differential in rats with A $\beta_{1-40}$ -induced Alzheimer disease given i.v.  $^{64}\text{Zn-asp}$ . Data are presented as median and IQR or as mean  $\pm$  SD. Data from different animal groups were compared using Kruskal–Wallis’s test or ANOVA with Tukey post-hoc test correspondingly. <sup>a</sup>— $p < 0.05$  as compared to intact animals; <sup>b</sup>— $p < 0.05$  as compared to sham-operated animals; <sup>c</sup>— $p < 0.05$  as compared to untreated animals with A $\beta_{1-40}$ -induced AD.

	Intact animals, n = 8	Sham-operated animals, n = 8	A $\beta_{1-40}$ -induced AD, n = 8	A $\beta_{1-40}$ -induced AD + $^{64}\text{Zn-asp}$ , n = 8
NLR	0.89 $\pm$ 0.4	0.68 $\pm$ 0.1 <sup>a</sup>	4.41 $\pm$ 0.1 <sup>ab</sup>	0.99 $\pm$ 0.1 <sup>c</sup>
LMR	8.31 $\pm$ 2.5	5.32 $\pm$ 1.8 <sup>a</sup>	20.46 $\pm$ 4.2 <sup>ab</sup>	6.45 $\pm$ 2.9 <sup>c</sup>
PLR	47.7 $\pm$ 16.3	44.3 $\pm$ 12.5	90 $\pm$ 27.7 <sup>ab</sup>	48.4 $\pm$ 21.7 <sup>c</sup>
PNR	4.2 $\pm$ 1.2	6.7 $\pm$ 2.2	19.6 $\pm$ 0.7 <sup>ab</sup>	6.3 $\pm$ 3.3 <sup>c</sup>
PMR	285.4 $\pm$ 92.4	245.5 $\pm$ 52.3	1887.5 $\pm$ 81.5 <sup>ab</sup>	335.3 $\pm$ 87.5 <sup>c</sup>
NMR	5.3 $\pm$ 2.5	3.6 $\pm$ 1.3 <sup>a</sup>	90 $\pm$ 16.8 <sup>ab</sup>	6.3 $\pm$ 3 <sup>c</sup>
SII	199.9 $\pm$ 45.4	264.2 $\pm$ 40.7 <sup>a</sup>	1760.9 $\pm$ 225.4 <sup>ab</sup>	250.8 $\pm$ 40.9 <sup>c</sup>
MPV/PLT	0.06 $\pm$ 0.01	0.03 $\pm$ 0.01 <sup>a</sup>	0.03 $\pm$ 0.01 <sup>a</sup>	0.05 $\pm$ 0.02 <sup>c</sup>

**Table 2.** Indices of systemic inflammation in rats with A $\beta_{1-40}$ -induced Alzheimer disease given i.v.  $^{64}\text{Zn-asp}$ . Data are presented as mean  $\pm$  SD. Data from different animal groups were compared using ANOVA with Tukey post-hoc test. <sup>a</sup> $p < 0.05$  as compared to intact animals; <sup>b</sup> $p < 0.05$  as compared to sham-operated animals; <sup>c</sup> $p < 0.05$  as compared to untreated animals with A $\beta_{1-40}$ -induced AD.

coupled with significant increase of absolute (by 4.7 times as compared to intact rats and 3 times – to sham-operated) and relative (by 2 times) Gr (neutrophil, Neu) count (Table 1). In AD rats given the  $^{64}\text{Zn-asp}$ , total WBC and Neu count were within the normal range. Monocytopenia in rats with A $\beta_{1-40}$ -induced AD, probably caused by Mo recruiting into the inflamed brain areas<sup>67,68</sup>, was another marker of systemic inflammation. In animals with AD received  $^{64}\text{Zn-asp}$ , monocytopenia was found to be absent. It should be noted that slight leukocytosis coupled with increased absolute lymphocyte (Ly) count, which were observed in sham-operated animals, can be attributed to the resolution of post-surgical low-grade inflammation.

Additionally, we also calculated commonly used systemic inflammatory indices based on the composition ratio of blood cell counts: NLR, LMR, PLR, PNR, PMR, NMR, SII and MPV/PLT (Table 2).

NLR values in rats with A $\beta_{1-40}$ -induced AD were ~ 5 times higher, LMR values—more than two times higher, NMR values—~ 17 times higher, and SII values—~ 9 times higher than corresponding values in control animals. This additionally indicates disproportion in Neu, Mo and Ly count and proves persistent systemic inflammation, which is characteristic for AD patients. In animals with AD given i.v.  $^{64}\text{Zn-asp}$ , all aforementioned indices of systemic inflammation did not exceed those in control groups.

Platelets (PLT) have been established as crucial regulators of inflammatory responses under different pathological conditions. PLT overactivation in the course of inflammation is followed by the development of thrombosis, atherosclerosis, and cardiovascular diseases<sup>69</sup>. PLT interact with Neu, Mo and Ly physically and by producing soluble mediators, and in such a way facilitate migration and functioning of these cells<sup>70</sup>. In our experiments, PLT count in AD rats was the same as in sham-operated animals and 1.8 times higher than in intact animals (Table 1). Mean PLT volume (MPV) did not differ significantly in animals from different groups (data are not shown). As a result, MPV/PLT ratio values in animals from sham and AD groups were lower as compared to intact animals. MPV can indicate either PLT activation or increased number of large sized PLT without their activation. In the light of this information, decreased MPV/PLT in animals with AD might indicate aberrant PLT functionality. In rats with A $\beta_{1-40}$ -induced AD given i.v.  $^{64}\text{Zn-asp}$ , MPV/PLT values were at the level of intact animals. At the same time, PLR values in rats with AD were twice as high as in control animals. PNR values in AD group were 4.7 times higher than in intact animals and 3 times higher than in sham-operated rats. PMR values in animals with AD were ~ 7 times higher as compared to those in control animals. This can additionally indicate improper PLT functioning. In AD rats received  $^{64}\text{Zn-asp}$ , all these indices were at the level of intact animals.

Additional sign of persistent systemic inflammation in our study was anemia of inflammation or chronic disease (AICD), which is characteristic for AD<sup>71</sup>. The presence of AICD was ascertained by corresponding red blood cell (RBC) indices (Table 3). Earlier, we registered reproducing AICD in A $\beta$ <sub>1-40</sub>-induced AD model<sup>49</sup>. In our current study, RBC count in AD rats was slightly lower than those in control animals (Table 3).

Hb level values in animals with A $\beta$ <sub>1-40</sub>-induced AD were 1.7 times higher as compared to those in control animals. The values of mean corpuscular hemoglobin (MHC) and the concentration of hemoglobin in RBC (MCHC) in AD rats were also higher than in control groups by 2 and 1.8 times correspondingly. Mean corpuscular volume (MCV) values did not differ significantly in animals from different groups, whereas RBC distribution width (RDW) values in animals from AD group were 1.5 times higher than in control groups. In rats with A $\beta$ <sub>1-40</sub>-induced AD given i.v. <sup>64</sup>Zn-asp, all aforementioned measures did not differ from those in intact animals.

### Anti-inflammatory effects of <sup>64</sup>Zn-asp correlate with spatial memory improvements, and is associated with reduced DN loss in rats with A $\beta$ 1-40-induced AD

Pro-inflammatory state of MG/BAM, as well as systemic inflammation in rats with A $\beta$ <sub>1-40</sub>-induced AD was associated with spatial learning/memory impairments, and DN loss.

Immunohistochemical analysis using TH as DN protein marker and a quick estimate Q for quantitative assessment, which are considered the gold standard for rodent models of neurodegenerative diseases<sup>72</sup> were used for evaluating hippocampal DN loss. TH expression level in hippocampal preparations of intact animals, assessed by Q values, was  $6.0 \pm 0.0$  points (Fig. 4A). In sham group, the staining intensity of TH-positive cells did not differ significantly from that of intact rats and Q value was  $7.0 \pm 1.7$  points (Fig. 4B). In AD rats, TH expression level was  $2.3 \pm 1.5$  points, which is almost three times less than in animals from control group and indicates DN loss (Fig. 4C). I.v. administration <sup>64</sup>Zn-asp resulted in an increase in the Q value to  $4.0 \pm 2.0$  points (Fig. 4D), to a greater extent due to an increase in the cell staining intensity, rather than their number, indicating protective effect of the preparation on hippocampal DA functions.

ELISA analysis of brain homogenates showed a trend toward increased A $\beta$ 40 levels in AD rats compared to intact and sham-operated animals, with median values of 46.8 vs. 18.5 and 17.3, respectively (Fig. 5). Intravenous administration of <sup>64</sup>Zn-asp led to a slight reduction in A $\beta$ 40 levels (median value 29.1) in AD rats. Due to substantial individual variability in the AD and AD + Zn animal groups, the observed differences did not reach statistical significance.

To assess spatial learning and spatial memory, two Barnes maze training sessions were performed: at the beginning of the experiment (Days 1–4), and on Days 28–31 (18 days after the surgery in sham and AD groups) (Fig. 6B). The first criterion for characterizing spatial learning and spatial memory, was short-term (working) spatial memory, which was assessed by the latency to find out the escape box (t1). The t1 values decreased over both training sessions in all animal groups, as was indicated by analogous learning curves (data are not shown). In the first probe trial (Day 5), t1 values were comparable for animals from all groups (Fig. 6A). At the subsequent probe trial on Day 32 (after the second (post-surgery) training session), t1 values in animals from control groups were lower as compared to those on Day 5, as evidenced by positive values of  $\Delta t_{1-5-32}$  (Fig. 6B), indicating positive effect of repeated spatial memory training on working memory formation. In rats from AD group, median values of t1 on Day 5 and Day 32 were identical, and  $\Delta t_{1-5-32}$  was 10 times lower than in controls indicating deterioration of working learning and memory in these animals. In AD animals given i.v. <sup>64</sup>Zn-asp, median value of t1 on Day 32 was 1.5 times lower as compared to that on Day 5, and did not differ significantly from those in control animals. Median value of  $\Delta t_{1-5-32}$  was positive and 2 times higher than that in untreated AD animals, which testifies to positive effect of the preparation on spatial learning.

Next criterion, the time spent near the entrance to closed target hole (t2), characterizes short-term cognitive flexibility. The less time the animal has been near the closed entrance to the escape box, the higher its level of cognitive flexibility (frontal cortex function), i.e., the animal more rapidly recognizes that the rescue hole should be looked for elsewhere. The t2 values were comparable for animals from all groups on Day 5 (after the first training session), and decreased by 30–50% in animals from control groups after the post-surgery training session (second probe trial, Day 32) as compared with values after the first training session (Day 5) (Fig. 6C), indicating positive effect of retraining on cognitive flexibility. Median values of  $\Delta t_{2-5-32}$  in these animals were > 0

	Intact animals, n = 8	Sham-operated animals, n = 8	A $\beta$ <sub>1-40</sub> -induced AD, n = 8	A $\beta$ <sub>1-40</sub> -induced AD + <sup>64</sup> Zn-asp, n = 8
RBC 10 <sup>6</sup> / $\mu$ l	7.3 $\pm$ 0.9	6.8 $\pm$ 0.4	6 $\pm$ 2	7 $\pm$ 0.3
Hgb, g/dl	15.8 $\pm$ 2.1	15.5 $\pm$ 1.4	27.1 $\pm$ 2.5 <sup>ab</sup>	14.1 $\pm$ 1.1 <sup>c</sup>
HCT, %	38.5 $\pm$ 4.6	34.9 $\pm$ 2.6	35.6 $\pm$ 9.8	35.9 $\pm$ 1 <sup>c</sup>
MCV, fl	52.9 $\pm$ 2.7	50.9 $\pm$ 1	58.4 $\pm$ 5	51 $\pm$ 1 <sup>c</sup>
MCH, pg	23 $\pm$ 1.3	21.9 $\pm$ 1	44.4 $\pm$ 3.2 <sup>ab</sup>	20 $\pm$ 0.7 <sup>c</sup>
MCHC, g/dl	43 $\pm$ 1.8	40.9 $\pm$ 1.5	74.2 $\pm$ 3.2 <sup>ab</sup>	39.2 $\pm$ 2.2 <sup>c</sup>
RDW, %	15.8 $\pm$ 0.6	16 $\pm$ 2.5	24.4 $\pm$ 4.4 <sup>ab</sup>	16.8 $\pm$ 1.4 <sup>c</sup>

**Table 3.** Red blood cell indices in rats with A $\beta$ <sub>1-40</sub>-induced Alzheimer disease given i.v. <sup>64</sup>Zn-asp. Data are presented as mean  $\pm$  SD. Data from different animal groups were compared using ANOVA with Tukey post-hoc test. <sup>a</sup> $p$  < 0.05 as compared to intact animals; <sup>b</sup> $p$  < 0.05 as compared to sham-operated animals; <sup>c</sup> $p$  < 0.05 as compared to untreated animals with A $\beta$ <sub>1-40</sub>-induced AD.

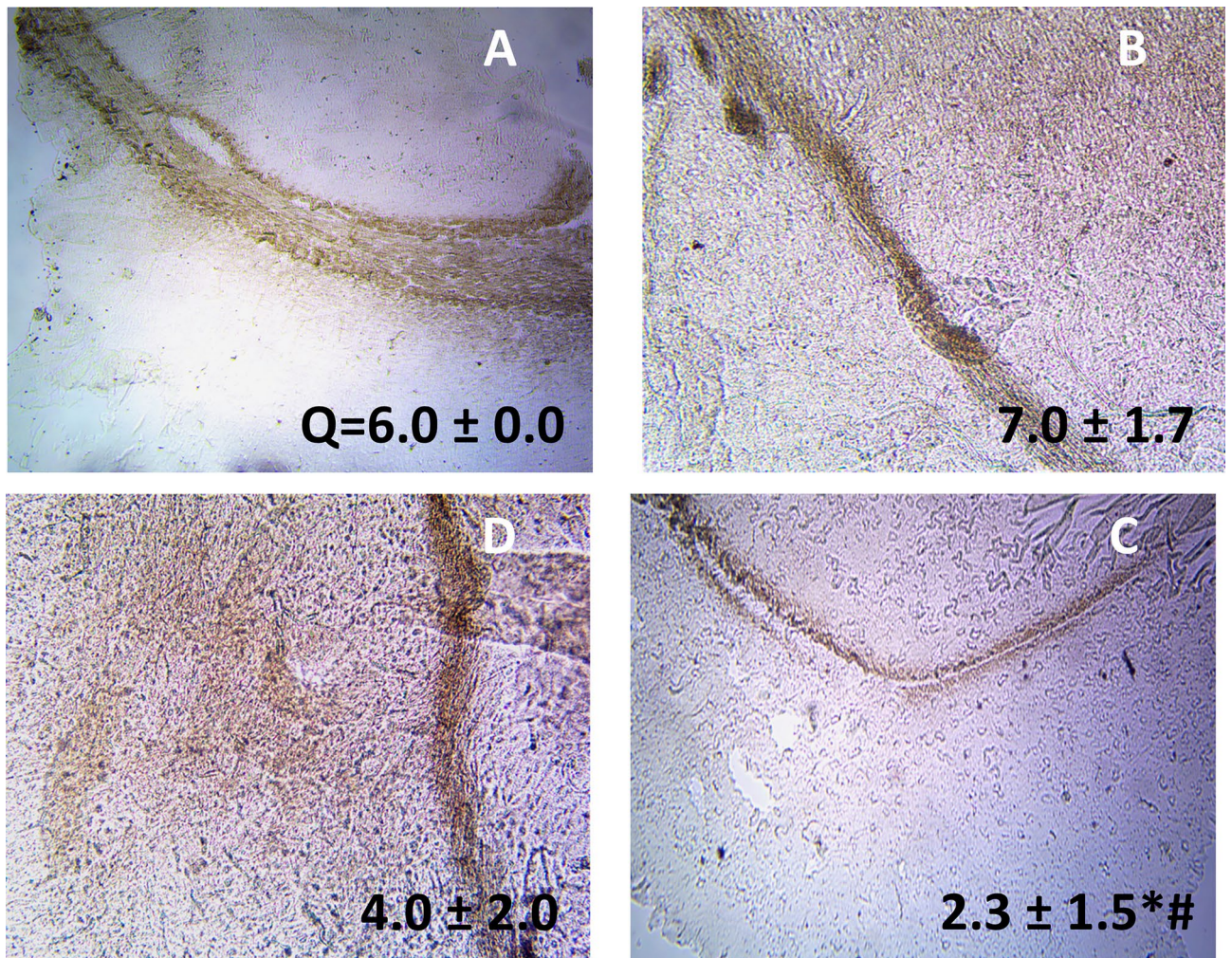


**Fig. 4.** Representative images of immunostaining of the TH-positive neurons (brown) in hippocampal area of the intact (A), sham-operated (B), AD (C) and AD + Zn experimental groups (Quick scores (Q) was calculated by multiplying the percentage of positive cells (P) by the intensity (I), magnification  $\times 400$ ). Data are presented as mean  $\pm$  SD. Data from intact, sham-operated, AD and AD + Zn animals were compared using ANOVA with Tukey post-hoc test. \* $p < 0.05$  as compared to intact animals; # $p < 0.05$  as compared to sham-operated animals.

(Fig. 6D). In contrast, in rats from AD group,  $\Delta t_{2_{5-32}} = -7$ , indicating increase time spent near the entrance to closed target hole even after retraining and impaired cognitive flexibility as a result of the disease development. Treatment AD rats with  $^{64}\text{Zn}$ -asp was associated with improvement of cognitive flexibility after the retraining; median value of  $\Delta t_{2_{5-32}}$  was positive and comparable to those in control animals. This can indicate positive impact of the  $^{64}\text{Zn}$ -asp treatment on the frontal lobe function of lesioned rats.

Our next measures were associated with remote spatial memory and behavioral flexibility. At the Day 9 (5th day after the last training in the first training session),  $t_1$  values were identical in animals from all four groups (Fig. 6E). At the Day 17 (13 days after the end of the first training session), a tendency to shortening  $t_1$  was observed in rats from control groups with positive  $\Delta t_{1_{9-17}}$  values (Fig. 6F), indicating memory consolidation. Whereas in rats with AD,  $t_1$  values were higher at this time point as compared to values five days after the first training session. It indicates, that A $\beta$  surgery and disease initiation held the week before, had negatively affected the remote spatial memory consolidation. Treatment with  $^{64}\text{Zn}$ -asp did not affect this parameter in AD animals.

At the Day 36 (5 days after the second (post-surgery) training session),  $t_1$  values in intact rats significantly decreased, indicating progressive improvement of remote spatial memory after retraining. In sham-operated rats,  $t_1$  values at the Day 36 were only a little lower than those at Day 9 (Fig. 6G), and were slightly higher as compared to Day 17 (Fig. 6H). This could be viewed as negative consequences of the placebo surgery, which interfere with forming of remote spatial memory. In rats with AD,  $t_1$  values at Day 36 did not differ significantly from those at Day 9 and Day 17, demonstrating deterioration of the remote spatial learning and memory. In AD rats given i.v.  $^{64}\text{Zn}$ -asp,  $t_1$  values at Day 36 were significantly lower as compared to those at Day 9 and Day 17, indicating improvement of remote spatial learning and memory.

The improvement of cognitive flexibility in the remote period after the first training session was observed in intact and sham-operated groups:  $t_2$  values at day 17 were significantly lower than those at the Day 9 (Fig. 6).

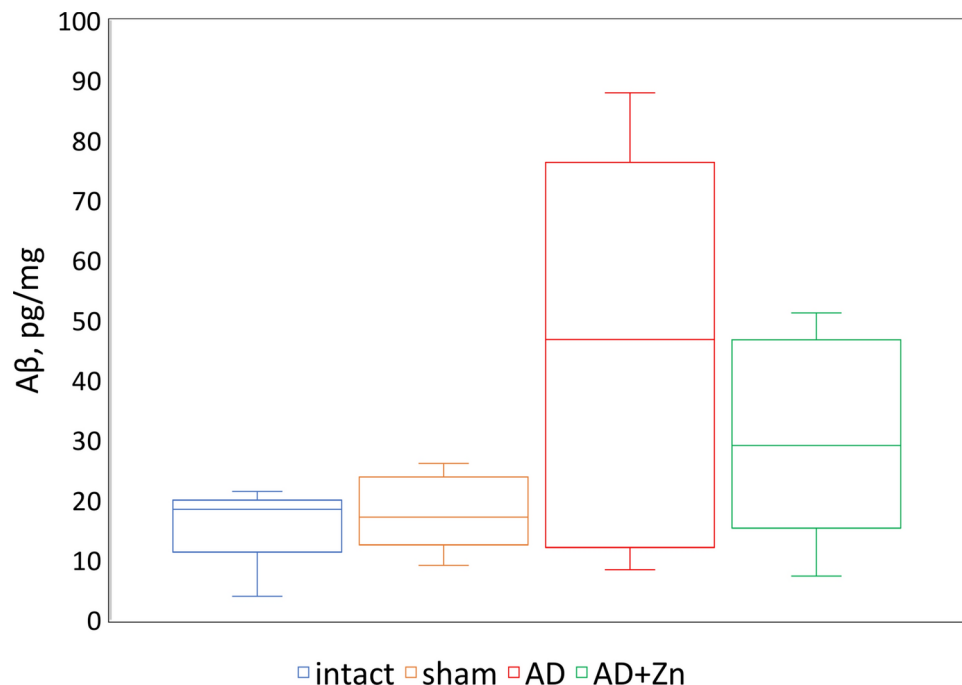


**Fig. 5.** The effect of i.v. administration with  $^{64}\text{Zn}$ -asp on  $\text{A}\beta_{40}$  levels in hippocampus of rats with  $\text{A}\beta_{1-40}$ -induced AD.

Unexpectedly, at Day 36 (after the second training session),  $t_2$  values in these groups returned to the level at the Day 9 (Fig. 6K), indicating that experience does not enhance remote cognitive flexibility in aged rats. In animals from AD group, cognitive flexibility in the remote period after retraining was significantly impaired:  $t_2$  median values at Day 36 were about 3 times higher than those at Day 9 (Fig. 6K) and Day 17 (Fig. 6L). Treatment with  $^{64}\text{Zn}$ -asp tended to a minor improvement of remote cognitive flexibility after retraining in AD rats.

Given the close link that exists between inflammation and cognitive impairment according to literature data<sup>73,74</sup>, we performed correlation analysis of the relationship between biomarkers of local and systemic inflammation and cognitive characteristics in animals with AD (Table 4).

The highest number of positive strong and very strong correlations<sup>75</sup> was registered between inflammatory biomarkers and measure of the working memory  $t_{1,32}$ . High values of this measure, which indicate deterioration of spatial learning and formation of short-term or working spatial memory, strongly correlated with markers of systemic inflammation (absolute and relative Gr count, relative Mo and Ly count, as well as values of systemic inflammation indices) and AICD, and quite strongly—with markers of pro-inflammatory MG/BAM activation (increased proportion of phagocytizing cells, high phagocytic activity and ROS generation as well as high level of CD86 and CD206 expression). This suggests that reducing local and systemic inflammation in rats with AD receiving i.v.  $^{64}\text{Zn}$ -asp, which was evidenced by normalizing the values of aforementioned biomarkers, can be one of the mechanisms of positive impact of the drug on working memory in lesioned animals.

Surprisingly, a measure of short-term cognitive flexibility  $t_{2\Delta_{5-32}}$  were more strongly correlated with biomarkers of systemic inflammation (absolute and relative Gr count, relative Mo and Ly count, as well as values of systemic inflammation indices), especially with AICD markers as compared with those of pro-inflammatory MG/BAM shift. This may indicate that counteracting the development of systemic inflammation and AICD can be one of the mechanisms of positive impact of  $^{64}\text{Zn}$ -asp i.v. administration on short-term cognitive flexibility in AD rats.

Measures of long-term or remote spatial learning/memory generally had weaker correlation with biomarkers of neuro- and systemic inflammation as compared to those of short-term learning/memory. Strongest correlation of  $t_{1,36}$  values, which indicate the ability of animals to improve spatial memory after retraining, was observed with MG/BAM ROS generation and CD206 expression level, as well as with Hb concentration values. Moderate correlation prevailed between the measure of remote spatial learning and memory formation  $t_{1\Delta_{9-36}}$  and biomarkers of local and systemic inflammation. Close relationships with this parameter were registered only for MG/BAM ROS generation and CD86 expression level, as well as for Hb concentration:  $r$  values  $-0.63$ ,  $-0.63$  and  $-0.68$  respectively. This indicates that pro-inflammatory MG/BAM metabolic shift with increased ROS production interferes with formation of remote spatial memory after retraining. Reducing pro-inflammatory MG/BAM shift by the i.v. treatment with  $^{64}\text{Zn}$ -asp can be one of the mechanisms preventing deterioration of spatial learning ability in lesioned rats.

Surprisingly, the highest number of correlations with spatial learning/memory was registered for Hb concentration among all biomarkers of inflammation. This emphasize newly described role of Hb in the AD pathogenesis, and suggests that decrease of plasma Hb level (as a component of systemic inflammation) in rats

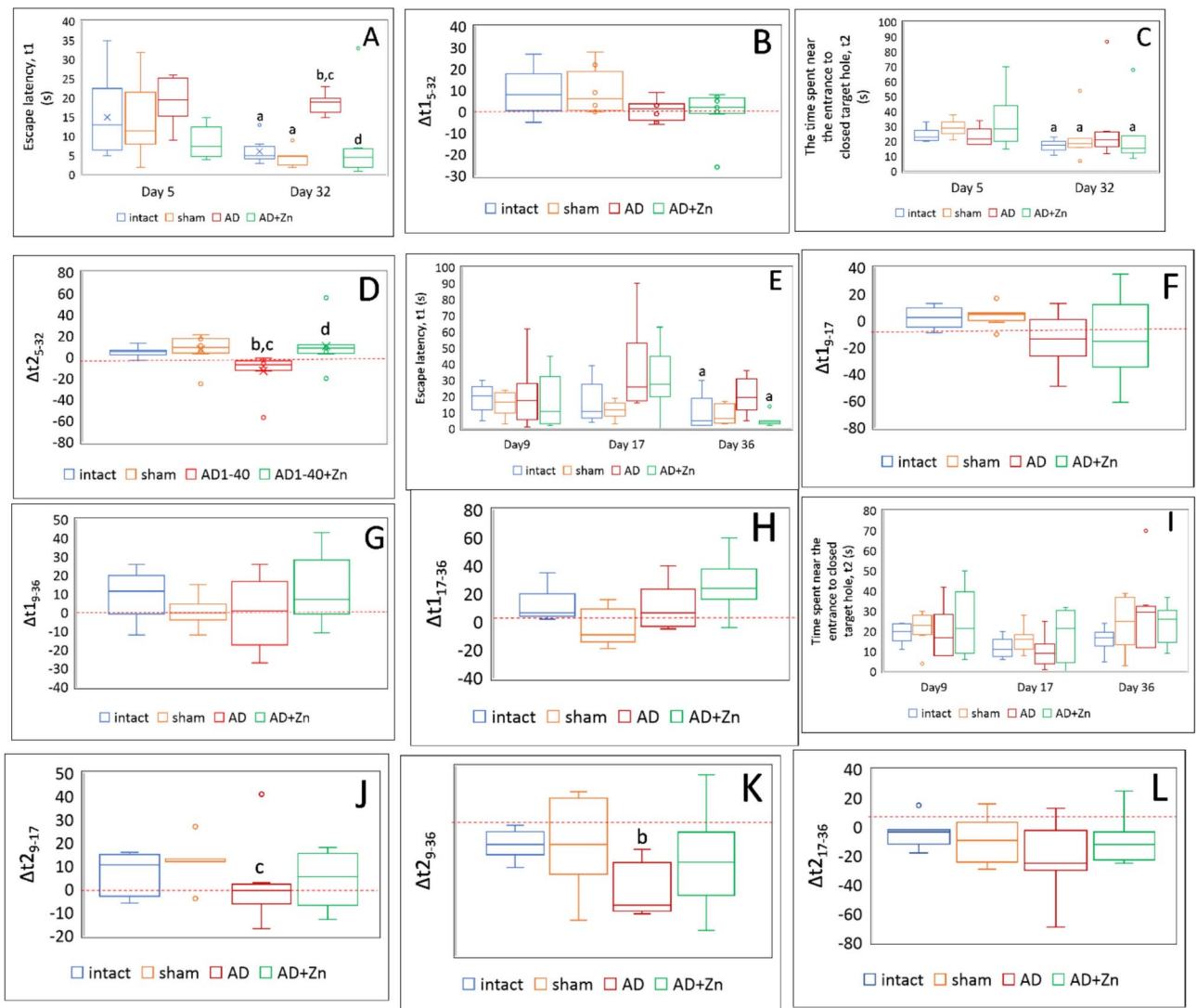


**Fig. 6.** The effect of i.v. administration with  $^{64}\text{Zn}$ -asp on behavioral characteristics of rats with  $\text{A}\beta_{1-40}$ -induced AD in the Barnes Maze Test. **A, B**—short-term spatial memory; **C, D**—short-term cognitive flexibility; **E, F, G and H**—remote spatial memory, **I, J, K and L**—remote cognitive flexibility.  $n = 8$  in each animal group. Data are presented as medians and IQR. Data from different animal groups were compared using Kruskal–Wallis’s test. <sup>a</sup> $p < 0.05$  as compared to the corresponding value at Day 5 (Fig. A and C) or Day 9 (Fig. E); <sup>b</sup> $p < 0.05$  as compared to the corresponding value in intact animals at the same time point; <sup>c</sup> $p < 0.05$  as compared to corresponding value in sham-operated animals at the same time point; <sup>d</sup> $p < 0.05$  as compared to corresponding value in untreated AD animals at the same time point.

with AD given i.v.  $^{64}\text{Zn}$ -asp can be one of the mechanisms of positive drug effect on cognitive parameters in lesioned animals.

Parameters of long-term (remote) cognitive flexibility virtually were not correlated with markers of neuro- and systemic inflammation.

## Discussion

In this study,  $\text{A}\beta_{1-40}$ -induced AD model was used for assessing impact of i.v. administration with  $^{64}\text{Zn}$ -asp on local and systemic inflammation, and cognitive parameters in rats. This model was selected because of three main reasons. First, unlike  $\text{A}\beta_{1-42}$ , whose accumulation is inherent for early onset familial AD,  $\text{A}\beta_{1-40}$  deposition is characteristic for late-onset AD, which is currently more common in the aging population worldwide, and it is these oligomers that prevail in the brain, blood vessels, and other tissues in patients with sporadic AD<sup>76</sup>. Second, since behavioral and pathological phenomena of AD, including neuro- and systemic inflammation are observed following  $\text{A}\beta_{1-40}$  injection into the hippocampus, the  $\text{A}\beta_{1-40}$ -induced model is generally regarded as an efficient model of AD<sup>49,77</sup>. Third, synaptic zinc has more impact on  $\text{A}\beta_{1-40}$  as compared to  $\text{A}\beta_{1-42}$ <sup>20</sup>.

The bioavailability and functional outcomes of zinc can be influenced by the form of Zn compound used. Zinc supplements progressed from inorganic to organic forms, partially, due to one of the key disadvantages of

	Short-term spatial learning/memory		Short-term cognitive flexibility		Remote spatial learning/memory			Remote cognitive flexibility	
	t1 <sub>32</sub>	t1 Δ <sub>5-32</sub>	t2 <sub>32</sub>	t2 Δ <sub>5-32</sub>	t1 <sub>36</sub>	t1 Δ <sub>9-17</sub>	t1 Δ <sub>9-36</sub>	t2 Δ <sub>9-36</sub>	t2 Δ <sub>17-36</sub>
<i>MG/BAM characteristics</i>									
PP, %	0.79	-0.53		-0.43	0.73		-0.52		
PI, MFI	0.76	-0.88		-0.41					
ROS, MFI	0.79			-0.49	0.85		-0.63		
CD86+, %								-0.46	
CD86, MFI	0.93	-0.71	0.43	-0.65	0.59				
CD206+, %	0.56				0.62		-0.46		
CD206, MFI	0.69		0.42	-0.55	0.84	-0.41	-0.63		
<i>Systemic inflammation markers</i>									
Gr, x 10 <sup>3</sup> /μl	0.93	-0.71		-0.65	0.62				
Mo, x 10 <sup>3</sup> /μl	-0.61	0.42			-0.41				
Ly, x 10 <sup>3</sup> /μl									
Gr, %	0.95	-0.70		-0.64	0.64				
Mo, %	-0.90	0.59		0.75	-0.48				
Ly, %	-0.95	0.71		0.60	-0.67				
NLR	0.93			-0.67	0.67		-0.41		
SII	0.84			-0.62					
PNR	0.93			-0.65	0.62		-0.49		
NMR	0.93			-0.67	0.64				
<i>AICD indicators</i>									
Hgb, g/dl	0.88		0.56	-0.67	0.86	-0.43	-0.68	-0.47	-0.53
MCH, pg	0.90		0.49	-0.74	0.61				
MCHC, g/dl	0.91		0.43	-0.70	0.70		-0.46		

**Table 4.** Correlations between cognitive parameters and biomarkers of local and systemic inflammation in rats with Aβ<sub>1-40</sub>-induced Alzheimer disease.

Red shading in cells indicates very strong correlation, blue - strong, green - moderate. t1, escape latency - the time required for the animal to find the entrance to the target escape box from when the animal is released from the starting cylinder (characterizes spatial learning and spatial memory - related to the function of the hippocampus); t2, the time spent near the entrance to closed target hole (characterizes cognitive flexibility - related to the function of the frontal cortex of the brain). MCH, mean corpuscular hemoglobin; MCHC, concentration of hemoglobin in red blood cells; MFI, mean fluorescence intensity; NLR, neutrophil to lymphocyte ratio; NMR, neutrophil to monocyte ratio; PI, phagocytosis index; PLR, platelet to lymphocyte ratio; PNR, platelet to neutrophil ratio; PP, phagocytosis percentage; ROS, reactive oxygen species; SII, systemic immune inflammation index.

inorganic zinc agents: low bioavailability<sup>78</sup>. Different from zinc supplements, the <sup>64</sup>Zn-asp used in this study uses light isotope <sup>64</sup>Zn enriched to exceed 99%, which appears to allow the amplification of known anti-inflammatory features of zinc by the isotope effects<sup>38</sup>. Additionally, the <sup>64</sup>Zn-asp used in this study has another advantage, since the chelate complex Zn<sup>2+</sup> with aspartic acid was shown to possess allogenic suppressive activity indicating the prospects for it using to control inflammatory immune responses<sup>79</sup>.

In our experiments, the i.v. administration of <sup>64</sup>Zn-asp have had potent inhibitory effect on neuroinflammation in rats with AD, since metabolic profile of complex MG/BAM population in AD rats received preparation was almost the same as that of control animals unlike pro-inflammatory shifted in untreated AD rats. Namely, <sup>64</sup>Zn-asp administration was accompanied by decrease of phagocytizing MG/BAM cell proportion and *S.aureus* phagocytosis intensity. *S. aureus* sensing and phagocytosis by MG/BAM cells involve nuclear factor kappa B (NF-κB) activation<sup>80</sup>. Increased NF-κB-dependent phagocytic activity, which was observed in rats with AD, is a marker of pro-inflammatory MG/BAM metabolic shift<sup>63</sup>. As mentioned above, zinc impedes NF-κB signaling<sup>32</sup>, that can be one of the mechanisms of the inhibitory effect of <sup>64</sup>Zn-asp administration on MG/BAM phagocytic activity in rats with AD. Decreased phagocytic activity in turn was strongly correlated with improvement of short-term and remote spatial learning/memory. Increased ROS generation is one of the key hallmarks of so-called disease-associated microglia (DAM) in neurodegenerative diseases including AD<sup>81</sup>. Aforementioned zinc antioxidant properties include inducing the expression of metallothioneins, activation of antioxidant proteins and enzymes etc.<sup>32</sup>. Oral zinc supplementation was shown is accompanied by alleviating oxidative stress in

inflammatory condition<sup>82,83</sup>. In our experiments, decreased ROS generation in rats with AD received i.v. <sup>64</sup>Zn-asp administration was also strongly correlated with improvement of short-term and remote spatial learning/memory. Elevated level of ROS generation is one of the potential molecular factors causing DN loss<sup>84</sup>. In addition, inflammatory mediators decrease release of dopamine<sup>85</sup>. Improvement of indicators for DN measuring observed in our study can be explained by alleviating neuroinflammation including decrease levels of inflammatory mediators such as ROS.

Levels of CD86 (or B7-2—co-stimulatory receptor responsible for antigen presentation and T-cell activation) are upregulated in pro-inflammatory activated M1 MG<sup>63</sup>, the same applies to BAM<sup>86</sup>. Zinc was shown to down-regulate co-stimulatory molecule expression and promotes tolerogenic phenotype in antigen-presenting cells<sup>87,88</sup>. In rats with AD given the <sup>64</sup>Zn-asp, decreased CD86 expression level in MG/BAM, which indicate anti-inflammatory cell shift, was strongly correlated not only with spatial learning/memory improvement but also with enhancement of cognitive flexibility. The same goes for CD206 expression level, which is the marker of reactive MG and pro-inflammatory shifted BAM<sup>65</sup>. Cognitive improvements in AD rats following treatment with anti-inflammatory agents have been reported by several research groups. For instance, Xie et al. (2021) observed a reduction in learning and memory dysfunction in AD rats following treatment with 8-hydroxyquinoline-resveratrol derivatives<sup>89</sup>. Similarly, El-Shiekh et al. (2020) highlighted the potent anti-inflammatory effects of anthocyanin-enriched extracts from two Hibiscus varieties, which were also associated with significant neuroprotection in AD rats<sup>90</sup>.

Neuroinflammation coupled with vascular pathology in AD are accompanied by blood–brain barrier (BBB) weakening and outflowing inflammatory mediators into the periphery with developing systemic inflammation<sup>91,92</sup>. In addition, AD in human unavoidably entails modifications of the hematopoietic system and hematopoietic maladaptation, which seems to be reproduced in the Aβ<sub>1-40</sub>-induced AD model<sup>49,93</sup>. In our experiments, three sets of signs prove the systemic inflammation phenomenon exists in rats with Aβ<sub>1-40</sub>-induced AD. First, deviations from the norm of routine hematological parameters: absolute and relative neutrophilia, relative lymphopenia, absolute and relative monocytopenia. Second, substantially increased values of indices of systemic inflammation, and third, the presence of ACID. In AD animals that received i.v. <sup>64</sup>Zn-asp administration, blood parameters returned to normal. In the inflammatory conditions, dietary zinc supplementation or administration by injection could reduce the enrollment and activity of Neu, in such a way ameliorating inflammation and tissue damage<sup>94,95</sup>. In our experiments, reduced systemic inflammation in rats with AD given the i.v. <sup>64</sup>Zn-asp was correlated with short-term spatial learning/memory improvement, and quite strongly—with enhancement of short-term cognitive ability. Therefore, <sup>64</sup>Zn-asp effects that lower systemic inflammation, could be considered as one of the mechanisms of improvement of measures of short-term memory and cognitive flexibility. Our findings are consistent with data of de Vargas et al.<sup>96</sup>, which observed anti-inflammatory effects of zinc supplementation in overweight or obese women coupled with enhance cognitive health.

The reduction of AICD manifestations in rats with AD after the i.v. <sup>64</sup>Zn-asp administration deserves special attention due to correlation with improved cognitive performance measures. Particularly, free Hg serum level, in rats with AD given the i.v. <sup>64</sup>Zn-asp, were strongly correlated with cognitive improvements. Both low and high Hb serum levels are associated with an increased risk of dementia, including AD, which may relate to differences in white matter integrity and cerebral perfusion<sup>97</sup>. In addition, extracellular Hb released from destroyed RBC may cause neurotoxicity and neurodegeneration, as well as the BBB weakening in AD<sup>98,99</sup>. In addition to well-known stimulatory impact to erythropoiesis<sup>100</sup>, zinc possess cytoprotective activity through stabilizing membrane proteins<sup>101</sup>, and decrease RBC osmotic fragility<sup>102</sup>. That might explain positive impact of i.v. <sup>64</sup>Zn-asp administration in animals with AD on serum level of free Hb as well as on other RBC measures which were correlated with cognitive improvements.

Despite a significant improvement in long-term (remote) spatial learning/memory and slight improvement in remote cognitive flexibility in rats with AD given the i.v. <sup>64</sup>Zn-asp as compared with untreated rats, we did not observe strong correlations between measures of remote cognitive activity and markers of neuro- and systemic inflammation. Perhaps the reason lies in different vulnerability of neurons from distinct brain parts to inflammatory mediators<sup>103</sup>. Right posterior parietal cortex and the right lateral prefrontal cortex are responsible for the processing of spatial working memory. Right medial temporal lobe, including the hippocampus, are implicated in long-term spatial memory, although hippocampus is always necessary to retrieve spatial information<sup>104</sup>. The lack of correlation between these cognitive measures and inflammatory markers could reflect the contribution of processes other than inflammation to cognitive impairment. Therefore, another reason for the absence of correlation between improvements in measures of remote spatial memory and inflammatory markers in rats with AD given <sup>64</sup>Zn-asp could be direct impact of the drug on neuron functions, as well as Aβ accumulation, aggregation, or removal in the brain. In our study, the increased expression of tyrosine hydroxylase in the hippocampus, along with the reduced concentration of the soluble form of beta-amyloid in AD animals following intravenous <sup>64</sup>Zn-asp administration, supports this hypothesis. Zinc ability to promote neurogenesis and its neuroprotective properties are well-documented<sup>105</sup>. Our hypothesis regarding the effect of <sup>64</sup>Zn-asp on Aβ deposition is based on the assumption that the light zinc isotope can displace heavier isotopes, along with existing evidence on the detrimental impact of heavy zinc isotopes on the chirality of biological macromolecules. This disruption may lead to the incorporation of D-amino acids into proteins<sup>106</sup>. The presence of D-enantiomers is known to alter a protein's primary structure, thereby affecting its function and biological activity, potentially contributing to the formation and accumulation of abnormal proteins characteristic of neurodegenerative diseases<sup>107</sup>. However, this hypothesis requires further experimental validation in future studies.

Recent reviews consolidate evidence on the potential efficacy of zinc therapy in relieving microglial-mediated neuroinflammation, as well as preventing and alleviating cognitive decline in AD patients within clinical settings<sup>105</sup>. One of the key advantages of zinc over other anti-inflammatory and neuroprotective agents is its exceptionally low toxicity. Zinc toxicity leading to severe health issues is a relatively rare occurrence in

humans<sup>109</sup>. One of the crucial zinc properties, which supports its clinical application as part of AD combination therapy, is its ability to stimulate metallothionein synthesis. According to the Metal Hypothesis of AD, disruptions in metal homeostasis—particularly involving iron, copper, and zinc—can alter the redox state, impair mitochondrial and autophagic function, and initiate neurodegenerative processes<sup>110</sup>. Zinc functional deficiency and reduced metallothionein synthesis led to an inability to regulate copper metabolism properly, resulting in elevated levels of non-ceruloplasmin-bound copper (free copper) in the blood—a hallmark of AD patients. This excess free copper crosses the BBB, increasing labile copper levels in the brain, which contributes to oxidative stress, neurotoxicity, and the misfolding and aggregation of A $\beta$  and tau—key pathological features of AD. Additionally, non-ceruloplasmin-bound copper promotes a pro-inflammatory shift in microglia and astroglia, further driving neuroinflammation<sup>111</sup>. It is noteworthy that most pronounced effect in these clinical trials was observed following the Zinc-hydrogenaspartate use<sup>112</sup>. Given the increased affinity of the lighter zinc isotope for cysteine, it can be inferred that it offers advantages over zinc compounds with a natural isotope distribution, particularly in stimulating metallothionein synthesis and restoring metal homeostasis. This further supports the rationale for using <sup>64</sup>Zn-asp in the combined therapy of Alzheimer's disease.

There were some limitations of this study. The first limitation is the lack of assessment of the effect of <sup>64</sup>Zn-asp on glutamatergic and cholinergic neurons in the cortex and hippocampus, which are more significantly affected in AD compared to the dopaminergic system. The second limitation pertains to the absence of an evaluation of the impact of <sup>64</sup>Zn-asp on A $\beta$  deposition in relation to its anti-inflammatory effects. Additionally, further research is needed to explore the impact of <sup>64</sup>Zn-asp on metal homeostasis, given its close association with key components of AD pathogenesis, including protein misfolding, neuroinflammation, and systemic inflammation.

## Conclusion

In summary, local, and systemic inflammation is considered as an important component of AD pathogenesis. Therefore, the search for drugs to counteract with inflammatory processes in AD is highly relevant, considering global prevalence of the disease. In our study, A $\beta$ <sub>1-40</sub>-induced AD in rats was associated with pronounced neuroinflammation, as ascertained by pro-inflammatory metabolic shift of MG/BAM cells, as well as with persistent systemic inflammation, which manifested by sharply increased values of WBC-based inflammatory biomarkers and AICD development. The findings of our study indicate that i.v. <sup>64</sup>Zn-asp administration led to potent inhibition of both neuro- and systemic inflammation, that confer a beneficial impact on cognition in lesioned animals. Despite the aforementioned limitations, the results of the current study support the potential of using <sup>64</sup>Zn-asp to mitigate inflammation and improve cognition in AD.

## Data availability

The data that support the findings of this study are available from the corresponding author, upon reasonable request.

Received: 7 January 2025; Accepted: 7 April 2025

Published online: 24 April 2025

## References

- Reiss, A. B. & Pinkhasov, A. Special issue “commemorative issue celebrating the 20th anniversary of the Alzheimer's foundation of America: Understanding and treating Alzheimer's disease”. *Medicina Kaunas* **60**, 712. <https://doi.org/10.3390/medicina60050712> (2024).
- DeTure, M. A. & Dickson, D. W. The neuropathological diagnosis of Alzheimer's disease. *Mol. Neurodegener.* **14**, 32. <https://doi.org/10.1186/s13024-019-0333-5> (2019).
- 2024 Alzheimer's disease facts and figures. (2024). *Alzheimers Dement* 20:3708–3821. <https://doi.org/10.1002/alz.13809>
- Liu, Y. et al. The interaction between ageing and Alzheimer's disease: Insights from the hallmarks of ageing. *Transl. Neurodegener* **13**, 7. <https://doi.org/10.1186/s40035-024-00397-x> (2024).
- Tomaskova, H., Kuhnova, J., Cimler, R., Dolezal, O. & Kuca, K. Prediction of population with Alzheimer's disease in the European Union using a system dynamics model. *Neuropsychiatr. Dis. Treat.* **12**, 1589–1598. <https://doi.org/10.2147/NDT.S107969> (2016).
- Zhang, J. et al. Recent advances in Alzheimer's disease: Mechanisms, clinical trials and new drug development strategies. *Signal Transduct. Target Ther.* **9**, 211. <https://doi.org/10.1038/s41392-024-01911-3> (2024).
- Islam, M. R., Rabbi, M. A., Hossain, T., Sultana, S. & Uddin, S. Mechanistic approach to immunity and immunotherapy of Alzheimer's disease: A review. *ACS Chem. Neurosci.* <https://doi.org/10.1021/acchemneuro.4c00360> (2024).
- Sharo, C., Zhai, T. & Huang, Z. Investigation of potential drug targets involved in inflammation contributing to Alzheimer's disease progression. *Pharmaceuticals (Basel)* **17**, 137. <https://doi.org/10.3390/ph17010137> (2024).
- Mintun, M. A. et al. Donanemab in early Alzheimer's disease. *N. Engl. J. Med.* **384**, 1691–1704. <https://doi.org/10.1056/NEJMoA2100708> (2021).
- Gyimesi, M., Okolicsanyi, R. K. & Haupt, L. M. Beyond amyloid and tau: Rethinking Alzheimer's disease through less explored avenues. *Open Biol.* **14**, 240035. <https://doi.org/10.1098/rsob.240035> (2024).
- Roy, R. G., Mandal, P. K. & Maroon, J. C. Oxidative stress occurs prior to amyloid A $\beta$  plaque formation and tau phosphorylation in Alzheimer's disease: Role of glutathione and metal ions. *ACS Chem. Neurosci.* **14**, 2944–2954. <https://doi.org/10.1021/acchemneuro.3c00486> (2023).
- Kalaria, R. N. Neuropathological diagnosis of vascular cognitive impairment and vascular dementia with implications for Alzheimer's disease. *Acta Neuropathol.* **131**, 659–685. <https://doi.org/10.1007/s00401-016-1571-z> (2016).
- Wiatrak, B., Jawień, P., Szlag, A. & Jęskowiak-Kossakowska, I. Does inflammation play a major role in the pathogenesis of Alzheimer's disease?. *Neuromol. Med.* **25**(3), 330–335. <https://doi.org/10.1007/s12017-023-08741-6> (2023).
- Kinney, J. W. et al. Inflammation as a central mechanism in Alzheimer's disease. *Alzheimers Dement (N. Y.)* **4**, 575–590. <https://doi.org/10.1016/j.trci.2018.06.014> (2018).
- Perry, V. H. & Teeling, J. Microglia and macrophages of the central nervous system: the contribution of microglia priming and systemic inflammation to chronic neurodegeneration. *Semin. Immunopathol.* **5**, 601–612. <https://doi.org/10.1007/s00281-013-0382-8> (2013).

16. Wu, S., Chen, N. & Wang, C. Frontiers and hotspots evolution in anti-inflammatory studies for Alzheimer's disease. *Behav. Brain Res.* **472**, 115178. <https://doi.org/10.1016/j.bbr.2024.115178> (2024).
17. Galloway, P., McMillan, D. C. & Sattar, N. Effect of the inflammatory response on trace element and vitamin status. *Ann. Clin. Biochem.* **37**, 289–297. <https://doi.org/10.1258/0004563001899429> (2000).
18. Portbury, S. D. & Adlard, P. A. Zinc signal in brain diseases. *Int. J. Mol. Sci.* **18**, 2506. <https://doi.org/10.3390/ijms18122506> (2017).
19. Coudray, C. et al. The effect of aging on intestinal absorption and status of calcium, magnesium, zinc, and copper in rats: A stable isotope study. *J. Trace Elem. Med. Biol.* **20**, 73–81. <https://doi.org/10.1016/j.jtemb.2005.10.007> (2006).
20. Xie, Z., Wu, H. & Zhao, J. Multifunctional roles of zinc in Alzheimer's disease. *Neurotoxicology* **80**, 112–123. <https://doi.org/10.1016/j.neuro.2020.07.003> (2020).
21. Craddock, T. J. et al. The zinc dyshomeostasis hypothesis of Alzheimer's disease. *PLoS ONE* **7**, e33552. <https://doi.org/10.1371/journal.pone.0033552> (2012).
22. Brewer, G. J. et al. Subclinical zinc deficiency in Alzheimer's disease and Parkinson's disease. *Am. J. Alzheimers Dis. Other Dement.* **25**(7), 572–575. <https://doi.org/10.1177/1533317510382283> (2010).
23. González, C. et al. Serum zinc, copper, insulin and lipids in Alzheimer's disease epsilon 4 apolipoprotein E allele carriers. *Eur. J. Clin. Invest.* **29**, 637–642. <https://doi.org/10.1046/j.1365-2362.1999.00471.x> (1999).
24. Rembach, A. et al. Decreased serum zinc is an effect of ageing and not Alzheimer's disease. *Metallomics Integr. Biometal Sci.* **6**(7), 1216–1219. <https://doi.org/10.1039/c4mt00060a> (2014).
25. Panayi, A. E., Spyrou, N. M., Iversen, B. S., White, M. A. & Part, P. Determination of cadmium and zinc in Alzheimer's brain tissue using inductively coupled plasma mass spectrometry. *J. Neurol. Sci.* **195**, 1–10. [https://doi.org/10.1016/s0022-510x\(01\)00672-4](https://doi.org/10.1016/s0022-510x(01)00672-4) (2002).
26. Religa, D. et al. Elevated cortical zinc in Alzheimer disease. *Neurology* **67**, 69–75. <https://doi.org/10.1212/01.wnl.0000223644.08653.b5> (2006).
27. Li, Q. & Barres, B. A. Microglia and macrophages in brain homeostasis and disease. *Nat Rev Immunol* **18**, 225–242. <https://doi.org/10.1038/nri.2017.125> (2018).
28. Kaur, S. K. M., Sharma, A., Giridharan, V. V. & Dandekar, M. P. Brain resident microglia in Alzheimer's disease: Foe or friends. *Inflammopharmacology* <https://doi.org/10.1007/s10787-024-01550-8> (2024).
29. Higashi, Y., Aratake, T., Shimizu, T., Shimizu, S. & Saito, M. Role of zinc in microglial phenotypes. *Metallomics Res.* **2**, 54–63. <https://doi.org/10.11299/metallomicsresearch.MR202116> (2022).
30. Wang, Y., Song, Y., Zhang, L. & Huang, X. The paradoxical role of zinc on microglia. *J. Trace Elem. Med. Biol.* **83**, 127380. <https://doi.org/10.1016/j.jtemb.2023.127380> (2024).
31. Fujie, T. et al. Zinc diethyldithiocarbamate as an inducer of metallothionein in cultured vascular endothelial cells. *J. Toxicol. Sci.* **41**(2), 217–224. <https://doi.org/10.2131/jts.41.217> (2016).
32. Jarosz, M., Olbert, M., Wyszogrodzka, G., Młyniec, K. & Librowski, T. Antioxidant and anti-inflammatory effects of zinc. Zinc-dependent NF- $\kappa$ B signaling. *Inflammopharmacology* **25**, 11–24. <https://doi.org/10.1007/s10787-017-0309-4> (2017).
33. Brewer, G. J. Copper excess, zinc deficiency, and cognition loss in Alzheimer's disease. *BioFactors* **38**, 107–113. <https://doi.org/10.1002/biof.1005> (2012).
34. Squitti, R. et al. Zinc therapy in early Alzheimer's disease: Safety and potential therapeutic efficacy. *Biomolecules* **10**, 1164. <https://doi.org/10.3390/biom10081164> (2020).
35. Jaouen, K. et al. Dynamic homeostasis modeling of Zn isotope ratios in the human body. *Metallomics* **11**, 1049–1059. <https://doi.org/10.1039/c8mt00286j> (2019).
36. Moynier, F. et al. Copper and zinc isotopic excursions in the human brain affected by Alzheimer's disease. *Alzheimers Dement (Amst.)* **12**, e12112. <https://doi.org/10.1002/dad2.12112> (2020).
37. Tanaka, Y. K. & Hirata, T. Stable isotope composition of metal elements in biological samples as tracers for element metabolism. *Anal. Sci.* **34**, 645–655. <https://doi.org/10.2116/analsci.18SBR02> (2018).
38. Solovyev, N. et al. Cu, Fe, and Zn isotope ratios in murine Alzheimer's disease models suggest specific signatures of amyloidogenesis and tauopathy. *J. Biol. Chem.* **296**, 100292. <https://doi.org/10.1016/j.jbc.2021.100292> (2021).
39. Albarede, F. et al. Medical applications of Cu, Zn, and S isotope effects. *Metallomics* **8**, 1056–1070. <https://doi.org/10.1039/c5mt00316d> (2016).
40. Novak, P., Balakin, A. & Temnik, M. In vitro anticancer activity of the light stable zinc isotope ( $^{64}\text{Zn}$ ) compounds. *Anticancer Res.* **42**, 5685–5698. <https://doi.org/10.21873/anticancer.16077> (2022).
41. Novak, P., Temnikov, M. & Balakin, O. US20200000845A1—Pharmaceutical Composition for Improving Health, Cure Abnormalities and Degenerative Disease, Achieve Anti-Aging Effect of Therapy and Therapeutic Effect on Mammals and Method Thereof - Google Patents (2022) <https://patents.google.com/patent/US20200000845A1/en>
42. Fukada, T., Yamasaki, S., Nishida, K., Murakami, M. & Hirano, T. Zinc homeostasis and signaling in health and diseases: Zinc signaling. *J. Biol. Inorgan. Chem. JBIC A Publ. Soc. Biol. Inorgan. Chem.* **16**(7), 1123–1134. <https://doi.org/10.1007/s00775-011-0797-4> (2011).
43. Cvijanovich, N. Z. et al. Safety and dose escalation study of intravenous zinc supplementation in pediatric critical illness. *JPEN J. Parenter. Enteral. Nutr.* **40**, 860–868. <https://doi.org/10.1177/0148607115572193> (2016).
44. Baltacı, S. B., Gümüş, H., Ünal, Ö., Acar, G. & Bayiroğlu, A. F. Zinc supplementation improves ZIP14 (SLC39A14) levels in cerebral cortex suppressed by icv-STZ injection. *Noro Psikiyatr Ars* **61**, 11–14. <https://doi.org/10.29399/npa.28426> (2024).
45. Gumus, H. et al. Zinc ameliorates Nogo-A receptor and osteocalcin gene expression in memory-sensitive rat hippocampus impaired by intracerebroventricular injection of streptozotocin. *Biol. Trace Elem. Res.* **201**, 3381–3386. <https://doi.org/10.1007/s12011-022-03410-4> (2023).
46. AVMA Guidelines for the Euthanasia of Animals: 2020 Edition. <https://www.avma.org/sites/default/files/2020-02/Guidelines-on-Euthanasia-2020.pdf>
47. Shi, X. et al. Rat hippocampal proteomic alterations following intrahippocampal injection of amyloid beta peptide (1–40). *Neurosci. Lett.* **500**, 87–91. <https://doi.org/10.1016/j.neulet.2011.06.009> (2011).
48. Berchenko, O. G., Levicheva, N. O., Bevzyuk, D. O. & Sokolik, V. V. The effect of miR-101 on the memory of rats with a model of Alzheimer's disease. *Regul. Mech. Biosyst* **11**, 354–359. <https://doi.org/10.15421/022054> (2020).
49. Nefodova, A. et al. Systemic inflammation in A $\beta$ 1-40-induced Alzheimer's disease model: New translational opportunities. *Brain Res.* **1837**, 148960. <https://doi.org/10.1016/j.brainres.2024.148960> (2024).
50. Irwin, M. R., Curay, C. M., Choi, S. & Kiyatkin, E. A. Basic physiological effects of ketamine-xylazine mixture as a general anesthetic preparation for rodent surgeries. *Brain Res.* **1804**, 148251. <https://doi.org/10.1016/j.brainres.2023.148251> (2023).
51. Gholipour, P., Komaki, A., Parsa, H. & Ramezani, M. Therapeutic effects of high-intensity interval training exercise alone and its combination with ecdysterone against amyloid beta-induced rat model of Alzheimer's disease: A behavioral, biochemical, and histological study. *Neurochem. Res.* **47**, 2090–2108. <https://doi.org/10.1007/s11064-022-03603-2> (2022).
52. Peris, L. R., Scheuber, M. I., Shan, H., Braun, M. M. & Schwab, M. E. Barnes maze test for spatial memory: A new, sensitive scoring system for mouse search strategies. *Behav. Brain Res.* **458**, 114730. <https://doi.org/10.1016/j.bbr.2023.114730> (2024).
53. Walsh, S., Finn, D. P. & Dowd, E. Time-course of nigrostriatal neurodegeneration and neuroinflammation in the 6-hydroxydopamine-induced axonal and terminal lesion models of Parkinson's disease in the rat. *Neuroscience* **175**, 251–261. <https://doi.org/10.1016/j.neuroscience.2010.12.005> (2011).

54. Pauletti, G. et al. Assessment of methods for tissue-based detection of the HER-2/neu alteration in human breast cancer: A direct comparison of fluorescence in situ hybridization and immunohistochemistry. *J. Clin. Oncol.* **18**, 3651–3664. <https://doi.org/10.1200/JCO.2000.18.21.3651> (2000).
55. Dubey, H., Gulati, K. & Ray, A. Amelioration by nitric oxide (NO) mimetics on neurobehavioral and biochemical changes in experimental model of Alzheimer's disease in rats. *Neurotoxicology* **66**, 58–65. <https://doi.org/10.1016/j.neuro.2018.03.001> (2018).
56. Ou-Yang, H. et al. Inflammation markers and the risk of hypertension in people living with HIV. *Front Immunol.* **14**, 1133640. <https://doi.org/10.3389/fimmu.2023.1133640> (2023).
57. Frank, M. G., Wieseler-Frank, J. L., Watkins, L. R. & Maier, S. F. Rapid isolation of highly enriched and quiescent microglia from adult rat hippocampus: Immunophenotypic and functional characteristics. *J. Neurosci. Methods* **151**, 121–130. <https://doi.org/10.1016/j.jneumeth.2005.06.026> (2006).
58. Oliynyk, Z. et al. Inflammatory hallmarks in 6-OHDA- and LPS-induced Parkinson's disease in rats. *Brain Behav. Immun. Health* **30**, 100616. <https://doi.org/10.1016/j.bbih.2023.100616> (2023).
59. Mishra, P. et al. Descriptive statistics and normality tests for statistical data. *Ann. Card Anaesth.* **22**, 67–72. [https://doi.org/10.4103/aca.aca\\_157\\_18](https://doi.org/10.4103/aca.aca_157_18) (2019).
60. Chan, Y. L. & Walmsley, R. Learning and understanding the Kruskal–Wallis one-way analysis-of-variance-by-ranks test for differences among three or more independent groups. *Phys. Ther.* **77**, 1755–1761. <https://doi.org/10.1093/ptj/77.12.1755> (1997).
61. Dermitzakis, I. et al. CNS border-associated macrophages: Ontogeny and potential implication in disease. *Curr. Issues Mol. Biol.* **45**, 4285–4300. <https://doi.org/10.3390/cimb45050272> (2023).
62. Silvin, A., Qian, J. & Ginhoux, F. Brain macrophage development, diversity and dysregulation in health and disease. *Cell Mol. Immunol.* **20**, 1277–1289. <https://doi.org/10.1038/s41423-023-01053-6> (2023).
63. Jurga, A. M., Paleczna, M. & Kuter, K. Z. Overview of general and discriminating markers of differential microglia phenotypes. *Front Cell Neurosci.* **14**, 198. <https://doi.org/10.3389/fncel.2020.00198> (2020).
64. Sun, R. & Jiang, H. Border-associated macrophages in the central nervous system. *J Neuroinflammation* **21**, 67. <https://doi.org/10.1186/s12974-024-03059-x> (2024).
65. Wen, W., Cheng, J. & Tang, Y. Brain perivascular macrophages: Current understanding and future prospects. *Brain* **147**, 39–55. <https://doi.org/10.1093/brain/awad304> (2024).
66. Kolaczowska, E. & Kubes, P. Neutrophil recruitment and function in health and inflammation. *Nat. Rev. Immunol.* **13**, 159–175. <https://doi.org/10.1038/nri3399> (2013).
67. Kratofil, R. M., Kubes, P. & Deniset, J. F. Monocyte conversion during inflammation and injury. *Arterioscler Thromb Vasc. Biol.* **37**, 35–42. <https://doi.org/10.1161/ATVBAHA.116.308198> (2017).
68. Orozco, S. L., Canny, S. P. & Hamerman, J. A. Signals governing monocyte differentiation during inflammation. *Curr. Opin. Immunol.* **73**, 16–24. <https://doi.org/10.1016/j.coi.2021.07.007> (2021).
69. Ludwig, N., Hilger, A., Zarbock, A. & Rossaint, J. Platelets at the crossroads of pro-inflammatory and resolution pathways during inflammation. *Cells* **11**, 1957. <https://doi.org/10.3390/cells11121957> (2022).
70. Margraf, A. & Zarbock, A. Platelets in inflammation and resolution. *J. Immunol.* **203**, 2357–2367. <https://doi.org/10.4049/jimmunol.1900899> (2019).
71. Andreev, A. et al. The association between anemia of chronic inflammation and Alzheimer's disease and related dementias. *J. Alzheimers Dis. Rep.* **4**, 379–391. <https://doi.org/10.3233/ADR-200178> (2020).
72. White, R. B. & Thomas, M. G. Moving beyond tyrosine hydroxylase to define dopaminergic neurons for use in cell replacement therapies for Parkinson's disease. *CNS Neurol. Disord. Drug Targets* **11**, 340–349. <https://doi.org/10.2174/187152712800792758> (2012).
73. Schmidt-Morgenroth, I., Michaud, P., Gasparini, F. & Avrameas, A. Central and peripheral inflammation in mild cognitive impairment in the context of Alzheimer's disease. *Int. J. Mol. Sci.* **24**, 10523. <https://doi.org/10.3390/ijms241310523> (2023).
74. Appleton, J. et al. Brain inflammation co-localizes highly with tau in mild cognitive impairment due to early-onset Alzheimer's disease. *Brain* <https://doi.org/10.1093/brain/awae234> (2024).
75. Papageorgiou, S. N. On correlation coefficients and their interpretation. *J. Orthod.* **49**, 359–361. <https://doi.org/10.1177/14653125221076142> (2022).
76. Zou, P., Ding, Y., Sha, Y., Hu, B. & Nie, S. Humanin peptides block calcium influx of rat hippocampal neurons by altering fibrogenesis of Aβ(1–40). *Peptides* **24**, 679–685. [https://doi.org/10.1016/s0196-9781\(03\)00131-1](https://doi.org/10.1016/s0196-9781(03)00131-1) (2003).
77. Park, J. et al. Adalimumab improves cognitive impairment, exerts neuroprotective effects and attenuates neuroinflammation in an Aβ<sub>1–40</sub>-injected mouse model of Alzheimer's disease. *Cytotherapy* **21**, 671–682. <https://doi.org/10.1016/j.jcyt.2019.04.054> (2019).
78. Liu, S., Wang, N., Long, Y., Wu, Z. & Zhou, S. Zinc homeostasis: An emerging therapeutic target for neuroinflammation related diseases. *Biomolecules* **13**, 416. <https://doi.org/10.3390/biom13030416> (2023).
79. Piacenza, F., Giacconi, R., Costarelli, L. & Malavolta, M. Preliminary comparison of fractional absorption of zinc sulphate, zinc gluconate, and zinc aspartate after oral supplementation in healthy human volunteers. *Nutrients* **15**, 1885. <https://doi.org/10.3390/nu15081885> (2023).
80. Zhu, F., Yue, W. & Wang, Y. The nuclear factor kappa B (NF-κB) activation is required for phagocytosis of staphylococcus aureus by RAW 264.7 cells. *Exp. Cell Res.* **327**, 256–263. <https://doi.org/10.1016/j.yexcr.2014.04.018> (2014).
81. Simpson, D. S. A. & Oliver, P. L. ROS generation in microglia: Understanding oxidative stress and inflammation in neurodegenerative disease. *Antioxidants (Basel)* **9**, 743. <https://doi.org/10.3390/antiox9080743> (2020).
82. Sun, X. et al. Zinc supplementation alleviates oxidative stress to inhibit chronic gastritis via the ROS/NF-κB pathway in a mouse model. *Food Funct.* **15**, 7136–7147. <https://doi.org/10.1039/d4fo01142b> (2024).
83. Mohammadi, H. et al. Effects of zinc supplementation on inflammatory biomarkers and oxidative stress in adults: A systematic review and meta-analysis of randomized controlled trials. *J. Trace Elem. Med. Biol.* **68**, 126857. <https://doi.org/10.1016/j.jtemb.2021.126857> (2021).
84. Delcambre, S., Nonnenmacher, Y. & Hiller, K. Dopamine metabolism and reactive oxygen species production. In *Mitochondrial mechanisms of degeneration and repair in Parkinson's disease* (ed. Buhlman, L.) 25–47 (Springer, Cham, 2016). [https://doi.org/10.1007/978-3-319-42139-1\\_2](https://doi.org/10.1007/978-3-319-42139-1_2).
85. Bekhat, M. et al. Functional connectivity in reward circuitry and symptoms of anhedonia as therapeutic targets in depression with high inflammation: Evidence from a dopamine challenge study. *Mol. Psychiatry* **27**, 4113–4121. <https://doi.org/10.1038/s41380-022-01715-3> (2022).
86. Gerganova, G., Riddell, A. & Miller, A. A. CNS border-associated macrophages in the homeostatic and ischaemic brain. *Pharmacol. Ther.* **240**, 108220. <https://doi.org/10.1016/j.pharmthera.2022.108220> (2022).
87. Hojyo, S. & Fukada, T. Roles of zinc signaling in the immune system. *J. Immunol. Res.* **2016**, 6762343. <https://doi.org/10.1155/2016/6762343> (2016).
88. George, M. M., Subramanian Vignesh, K., Landero Figueroa, J. A., Caruso, J. A. & Deepe, G. S. Jr. Zinc induces dendritic cell tolerogenic phenotype and skews regulatory T Cell-Th17 balance. *J. Immunol.* **197**, 1864–1876. <https://doi.org/10.4049/jimmunol.1600410> (2016).
89. Xie, J., Su, R., Wu, D., Qin, Y. & Yun, X. A novel synthetic compound shows antioxidant and anti-inflammatory activity and alleviates cognitive deficits in rats for the treatment of Alzheimer's disease. *Ann. Palliative Med.* **10**(9), 9508–9515. <https://doi.org/10.21037/apm-21-1983> (2021).

90. El-Shiekh, R. A., Ashour, R. M., Abd El-Haleim, E. A., Ahmed, K. A. & Abdel-Sattar, E. *Hibiscus sabdariffa* L.: A potent natural neuroprotective agent for the prevention of streptozotocin-induced Alzheimer's disease in mice. *Biomed. Pharmacother. Biomed. Pharmacother.* **128**, 110303. <https://doi.org/10.1016/j.biopha.2020.110303> (2020).
91. Cao, W. & Zheng, H. Peripheral immune system in aging and Alzheimer's disease. *Mol. Neurodegener.* **13**, 51. <https://doi.org/10.1186/s13024-018-0284-2> (2018).
92. Chen, T. et al. Cellular and molecular mechanisms of the blood–brain barrier dysfunction in neurodegenerative diseases. *Fluids Barriers CNS* **21**, 60. <https://doi.org/10.1186/s12987-024-00557-1> (2024).
93. Naert, G. & Rivest, S. A deficiency in CCR2+ monocytes: The hidden side of Alzheimer's disease. *J. Mol. Cell Biol.* **5**, 284–293. <https://doi.org/10.1093/jmcb/mjt028> (2013).
94. Shao, Y. R., Xu, D. Y. & Lin, J. Nutrients and rheumatoid arthritis: From the perspective of neutrophils. *Front Immunol.* **14**, 1113607. <https://doi.org/10.3389/fimmu.2023.1113607> (2023).
95. Lay, C. S. V. et al. Dietary zinc intake and absolute lymphocyte counts in advanced stage of nasopharyngeal cancer patients. *Hum. Nutr. Metab.* **36**, 200261. <https://doi.org/10.1016/j.hnm.2024.200261> (2024).
96. de Vargas, L. D. S. et al. Effects of zinc supplementation on inflammatory and cognitive parameters in middle-aged women with overweight or obesity. *Nutrients* **15**, 4396. <https://doi.org/10.3390/nu15204396> (2023).
97. Wolters, F. J. et al. Hemoglobin and anemia in relation to dementia risk and accompanying changes on brain MRI. *Neurology* **93**, e917–e926. <https://doi.org/10.1212/WNL.0000000000008003> (2019).
98. Drvenica, I. T., Stanić, A. Z., Maslovarić, I. S., Trivanović, D. I. & Ilić, V. L. Extracellular hemoglobin: Modulation of cellular functions and pathophysiological effects. *Biomolecules* **12**, 1708. <https://doi.org/10.3390/biom12111708> (2022).
99. Altinoz, M. A. et al. Involvement of hemoglobins in the pathophysiology of Alzheimer's disease. *Exp. Gerontol.* **126**, 110680. <https://doi.org/10.1016/j.exger.2019.110680> (2019).
100. Takahashi, A. Zinc supplementation enhances the hematopoietic activity of erythropoiesis-stimulating agents but not hypoxia-inducible factor–prolyl hydroxylase inhibitors. *Nutrients* **16**, 520. <https://doi.org/10.3390/nu16040520> (2024).
101. Perera, M. et al. Zinc preconditioning provides cytoprotection following iodinated contrast media exposure in in vitro models. *Contrast. Media Mol. Imaging* **2021**, 6686803. <https://doi.org/10.1155/2021/6686803> (2021).
102. Candan, F., Gültekin, F. & Candan, F. Effect of vitamin C and zinc on osmotic fragility and lipid peroxidation in zinc-deficient haemodialysis patients. *Cell Biochem. Funct.* **20**, 95–98. <https://doi.org/10.1002/cbf.947> (2002).
103. Wang, X., Michaelis, M. L. & Michaelis, E. K. Functional genomics of brain aging and Alzheimer's disease: Focus on selective neuronal vulnerability. *Curr. Genomics* **11**, 618–633. <https://doi.org/10.2174/138920210793360943> (2010).
104. Zorzo, C., Arias, J. L. & Méndez, M. Functional neuroanatomy of allocentric remote spatial memory in rodents. *Neurosci. Biobehav. Rev.* **136**, 104609. <https://doi.org/10.1016/j.neubiorev.2022.104609> (2022).
105. Li, Z., Liu, Y., Wei, R., Yong, V. W. & Xue, M. The important role of zinc in neurological diseases. *Biomolecules* **13**(1), 28. <https://doi.org/10.3390/biom13010028> (2022).
106. Soai, K. Asymmetric autocatalysis. Chiral symmetry breaking and the origins of homochirality of organic molecules. *Proc. Jpn. Acad. Ser. B Phys. Biol. Sci.* **95**(3), 89–110. <https://doi.org/10.2183/pjab.95.009> (2019).
107. Abdulbagi, M., Wang, L., Siddig, O., Di, B. & Li, B. D-amino acids and D-amino acid-containing peptides: Potential disease biomarkers and therapeutic targets?. *Biomolecules* **11**(11), 1716. <https://doi.org/10.3390/biom11111716> (2021).
108. Adlard, P. A. & Bush, A. I. Metals and Alzheimer's disease: How far have we come in the clinic?. *J. Alzheimer's Dis. JAD* **62**(3), 1369–1379. <https://doi.org/10.3233/JAD-170662> (2018).
109. Plum, L. M., Rink, L. & Haase, H. The essential toxin: Impact of zinc on human health. *Int. J. Environ. Res. Public Health* **7**(4), 1342–1365. <https://doi.org/10.3390/ijerph7041342> (2010).
110. Bush, A. I. & Tanzi, R. E. Therapeutics for Alzheimer's disease based on the metal hypothesis. *Neurother. J. Am. Soc. Exp. Neurother.* **5**(3), 421–432. <https://doi.org/10.1016/j.nurt.2008.05.001> (2008).
111. Brewer, G. J. & Kaur, S. Zinc deficiency and zinc therapy efficacy with reduction of serum free copper in Alzheimer's disease. *Int. J. Alzheimer's Dis.* **2013**, 586365. <https://doi.org/10.1155/2013/586365> (2013).
112. Squitti, R. et al. Zinc therapy in early Alzheimer's disease: Safety and potential therapeutic efficacy. *Biomolecules* **10**(8), 1164. <https://doi.org/10.3390/biom10081164> (2020).

## Author contributions

MT: supervision and writing—review and editing. MR: methodology, investigation, formal analysis. AB: methodology, conceptualization, and project administration. SG: conceptualization, writing—review and editing. TD: methodology, investigation. RB: methodology, conceptualization. ND: methodology, investigation. GT: supervision and writing—review and editing. LS: methodology, conceptualization, project administration and writing—original draft. All authors read the final version of the manuscript.

## Funding

The study was supported by a TSNUK project N 19DP036-03.

## Declarations

## Competing interests

The authors declare no competing interests.

## Additional information

**Correspondence** and requests for materials should be addressed to M.R.

**Reprints and permissions information** is available at [www.nature.com/reprints](http://www.nature.com/reprints).

**Publisher's note** Springer Nature remains neutral with regard to jurisdictional claims in published maps and institutional affiliations.

**Open Access** This article is licensed under a Creative Commons Attribution-NonCommercial-NoDerivatives 4.0 International License, which permits any non-commercial use, sharing, distribution and reproduction in any medium or format, as long as you give appropriate credit to the original author(s) and the source, provide a link to the Creative Commons licence, and indicate if you modified the licensed material. You do not have permission under this licence to share adapted material derived from this article or parts of it. The images or other third party material in this article are included in the article's Creative Commons licence, unless indicated otherwise in a credit line to the material. If material is not included in the article's Creative Commons licence and your intended use is not permitted by statutory regulation or exceeds the permitted use, you will need to obtain permission directly from the copyright holder. To view a copy of this licence, visit <http://creativecommons.org/licenses/by-nc-nd/4.0/>.

© The Author(s) 2025